63-14

FOREWORD

This is Scripps Institution of Oceanography Reference Report No. 63-14 prepared as the Final Report under Air Force Contract AF 33(657)-7739. It describes the results of a field experiment conducted with the Visibility Laboratory's instrumented trailer at Wright-Patterson Air Force Base, Ohio, during August and September 1962. The experiments were conducted under the technical supervision of S. Q. Duntley, J. I. Gordon, A. R. Boileau, R. W. Austin, and R. W. Johnson. A field party, including A. R. Boileau, R. W. Johnson, S. Lindroth, and K. W. McMaster placed the photometric apparatus in operation after the trailer had been transported by the Air Force to Wright-Patterson Air Force Base. S. Lindroth operated the apparatus throughout the data-taking period with the assistance of Master Sargent Edward Hart and Airmen Michael Murray and John Myers attached to the Reconnaissance Laboratory, ASD. Photometric calibrations were performed by R. W. Johnson who visited the experimental site from time to time throughout the course of the work. Data reduction was under the direction of J. I. Gordon assisted by P. E. Church, R. M. Kraft, D. M. Resch, A. L. Shaules, and J. W. Wasserboehr. The report was written by S. Q. Duntley.

ABSTRACT

Vertical ground-to-space beam transmittance, path radiance, and contrast transmittance for green light was measured from a ground station at Wright-Patterson Air Force Base, Ohio, on ten occasions during August and September 1962. On each occasion a Reconnaissance Laboratory photographic airplane photographed a pattern of white, grey, and black targets on the ground adjacent to the Visibility Laboratory equipment. The targets were radiometrically monitored by Cornell Aeronautical Laboratory in such a manner that target-to-aircraft beam transmittance, path radiance, and contrast transmittance could be obtained from the aerial photographs. The intended purpose of this joint experiment is a comparison of the target-to-space data predicted by the ground-based instruments with the ground-to-aircraft photographic data. The ground-based data are presented in this report, but comparison with the aerial data must await the completion of data reduction from the aerial photographs by Cornell Aeronautical Laboratory.

30 January 1963

GROUND-BASED MEASUREMENTS OF EARTH-TO-SPACE BEAM TRANSMITTANCE, PATH RADIANCE, AND CONTRAST TRANSMITTANCE

1. INTRODUCTION

The apparent contrast of objects on the surface of the earth as seen by astronauts or by satellite-borne cameras can be measured only from outside the atmosphere, although data obtained from very high altitude aircraft often provide a close approximation. No means have been available, however, for ascertaining this type of information through the use of ground-based instrumentation, but the possibility of an indirect method for achieving that capability has recently resulted from a study of satellite technology in progress at the Visibility Laboratory under a U. S. Navy Contract (NObs-84075).

A full account of the theory and the experimental data which underlie the proposed new method are presented in a report which was issued during January 1963 under Contract NObs-84075; that document, identified as Scripps Institution of Oceanography Reference No. 63-2, is appended to this report as an Appendix. Attempts on the part of the Visibility Laboratory to test the new method by means of data from high altitude balloons and from instrumented rockets were frustrated by weather and by malfunction of the rocket equipment. An account of these fruitless attempts is given on pages 8 and 9 of the Appendix.

An apparently successful series of tests was made, however, under Contract AF 33(657)-7739 with the Reconnaissance Laboratory of the

Aeronautical Systems Division of the U. S. Air Force during the summer of 1962; the results are presented in this, the Final Report under Contract AF 33(657)-7739. Advantage was taken of an ongoing Reconnaissance Laboratory project under which an Air Force photographic airplane made routine high altitude photographs of black, grey, and white panels situated on the athletic field near the Reconnaissance Laboratory at Wright-Patterson Air Force Base, Ohio. Under an Air Force contract with the Cornell Aeronautical Laboratory, Inc., photographic and photoelectric monitoring was provided at the panels during the flights so that measurements of beam transmittance, path radiance, and various forms of contrast transmittance from ground to air might be obtained from the aerial photographs.

The Air Force transported the Visibility Laboratory's instrumented trailer van to Wright-Patterson Air Force Base where it was placed alongside the target panels and manned jointly by Visibility Laboratory and Air Force personnel throughout a series of 11 flights during the period 16 August 1962 through 12 September 1962. Photoelectric measurements of solar transmittance, sky radiance, and ground irradiance were made simultaneously with the high altitude passes of the photographic airplane. This was accomplished in terms of green light selected by a combination of filters which matched the spectral sensitivity of the photoelectric photometers to that of a film-filter combination specified by the Reconnaissance Laboratory as that used in the aerial cameras. Reduction of the photoelectric data was carried out at the Visibility Laboratory. The results are presented in tabular form in this report.

Terrain reflectance measurements made photographically from the airplane at the time of the flights have been furnished by Cornell Aeronautical Laboratory. These values of reflectance have been combined with ground irradiance data to provide values of terrain radiance which, in combination with the beam transmittance and path radiance for the downward vertical paths of sight from ground to space, enabled values of ground-to-space contrast transmittance for objects seen against this background to be calculated. Predicted contrast transmittance values for a black background and a white background are also tabulated.

Comparison of the separate values of ground-to-space beam transmittance and path radiance as predicted from the ground-based measurements with measured values of ground-to-aircraft beam transmittance and path radiance obtained by means of aerial photography has not been possible because reduction of the photographic data for the flights has not yet been completed by the Cornell Aeronautical Laboratory.

2. THEORY

The theory which underlies the experiments described in this report was developed previously under U. S. Navy Contract NObs-84075; its derivation is fully described in a NObs-84075 report (SIO Ref. 63-2), copies of which are incorporated in this report as an Appendix. This Appendix provides a detailed description of the notation used by the Visibility Laboratory and a full discussion of the concepts which underlie each of the quantities which appear in the equations. In view of

the completeness of the Appendix, it will suffice to repeat in this section only those equations around which the experiments were designed. Definitions of the symbols employed in these equations are given despite the fact that they are also defined in the Appendix.

Altitude Designations

The ground targets and the Visibility Laboratory instrumentation at Wright-Patterson Air Force Base were located at an altitude of 750 feet above sea level. Target altitude is denoted in the following equations by the symbol z_t; thus $z_t = 750$ feet. The downward inclined path of sight begins at the target and extends upward to an observer who is assumed to be at some orbital altitude outside the atmosphere of the earth. The exact altitude of such an observer does not affect the apparent contrast, the path radiance, or the beam transmittance of the path of sight since, in all cases, the observer is beyond the atmosphere; the symbol ∞ is used throughout the following equations to denote this fact.

Contrast Transmittance

Equation (2) from page 3 of the Appendix can be written

$$\frac{C_\infty(\infty,\theta,\phi)}{C_o(z_t,\theta,\phi)} = \frac{{}_bN_o(z_t,\theta,\phi)\ T_\infty(\infty,\theta)}{{}_bN_o(z_t,\theta,\phi)\ T_\infty(\infty,\theta) + N^*_\infty(\infty,\theta,\phi)} \equiv {}_b\tau_\infty(\infty,\theta,\phi) \qquad (1)$$

where:

$C_{\infty}(\infty,\theta,\phi)$ represents the apparent contrast of the target as seen from outside the atmosphere along a downward inclined path* of sight having zenith angle θ and azimuth angle ϕ,

$C_o(z_t,\theta,\phi)$ represents the inherent contrast of the target located at terrain elevation z_t along a downward inclined path of sight having zenith angle θ and azimuth angle ϕ,

${}_bN_o(z_t,\theta,\phi)$ is the inherent radiance of the background against which the target is viewed along the downward path of sight θ,ϕ,

$N^*_{\infty}(\infty,\theta,\phi)$ is the path radiance of the downward inclined path of sight θ,ϕ from the target to any altitude outside the atmosphere (∞); it is partially dependent upon the surround of the target and background complex,

$T_{\infty}(\infty,\theta)$ is the beam transmittance for the downward inclined path of sight θ,ϕ from the target to any altitude outside the atmosphere (∞),

*The post-subscript refers to the path length from target to observer; the first modifier enclosed by parentheses specifies the altitude of the observer. Thus, $C_{1,250}(2,000,\pi)$ denotes the apparent contrast of a target located 1,250 feet directly beneath an observer at an altitude of 2,000 feet; since azimuth (ϕ) is indeterminant for a vertical path of sight, it is omitted. If the same target were viewed from 2,000 feet along a path of sight inclined downward at a zenith angle of 135° in a direction at right angles to the plane of the sun, the path length would be $1,250\sqrt{2} = 1,770$ feet and the apparent contrast would be written $C_{1,770}(2,000,135,90)$; the corresponding inherent contrast is written $C_o(750,135,90)$.

${}_b\mathcal{T}_{\infty}(\infty,\theta,\phi)$ is the (universal) contrast transmittance for the downward inclined path of sight θ,ϕ from the target to any altitude outside the atmosphere (∞).

The right-hand member of Eq. (1) is called the (universal) contrast transmittance because it specifies the contrast reducing property of the atmosphere from ground to space along the downward inclined path of sight θ,ϕ for <u>any</u> target which may be presented against the background. This universal property of the contrast transmittance is a result of the definitions which have been adopted for inherent and apparent contrast. In Eq. (1), inherent and apparent contrast are defined by Eqs. (2) and (3), respectively, as follows:

$$C_{\infty}(\infty,\theta,\phi) = \frac{{}_tN_{\infty}(\infty,\theta,\phi) - {}_bN_{\infty}(\infty,\theta,\phi)}{{}_bN_{\infty}(\infty,\theta,\phi)} \quad , \tag{2}$$

and

$$C_o(z_t,\theta,\phi) = \frac{{}_tN_o(z_t,\theta,\phi) - {}_bN_o(z_t,\theta,\phi)}{{}_bN_o(z_t,\theta,\phi)} \quad , \tag{3}$$

where

${}_tN_{\infty}(\infty,\theta,\phi)$ and ${}_bN_{\infty}(\infty,\theta,\phi)$ are the apparent radiance of the target and its background, respectively, as viewed from any point outside the atmosphere (∞) along the downward inclined path of sight θ,ϕ,

and

$_{t}N_{o}(z_{t},\theta,\phi)$ and $_{b}N_{o}(z_{t},\theta,\phi)$ are the inherent radiance of the target and its background, respectively, as viewed from zero distance along the downward inclined path of sight θ,ϕ.

The inherent radiance of the target and the inherent radiance of the background for the downward inclined path of sight θ,ϕ can either be measured directly at ground level by means of a telephotometer or they can be calculated by forming the product of irradiance and reflectance and dividing it by π. If the latter course is adopted, care should be exercised in obtaining appropriate values of reflectance because no known surface obeys "Lambert's Law of Reflection" completely and the directional reflective properties of man-made and natural objects are interwoven with the geometry and distribution of natural lighting in so complicated a manner that gross errors may result unless a reflectance applicable to the particular path of sight and the particular phase of natural lighting involved is accurately known. This is tantamount to the statement that only directly measured inherent radiance values in the direction of the path of sight are valid inputs to Eqs. (1) and (3). Fortunately, convenient portable telephotometers in both visual and photoelectric models are commercially available so that the direct measurement of the inherent radiance properties of target and background for the path of sight of interest can be measured readily.

Beam Transmittance

The beam transmittance for the path of sight depends upon the zenith angle Θ but not upon the azimuth angle $\emptyset$ except in unusual circumstances when gross horizontal non-uniformities exist in an asymmetric manner with respect to the location of the target. In such an instance, which fortunately is rare, little can be done to obtain a valid value for the beam transmittance. Ordinarily, however, the beam transmittance called for by Eq. (1) can be measured quite simply by means of a solar transmissometer. One such instrument is described and pictured in the Appendix. (See Appendix, Fig. 1.) This was the instrument used during the experiments to be described in this report.

Path Radiance

The path radiance called for by Eq. (1) can be determined for downward inclined paths of sight by a specially instrumented aircraft but it cannot be measured directly from the ground. An indirect method for obtaining this value from ground-based measurements is described, however, in the Appendix. Equation (9) on page 7 of the Appendix (SIO Ref. Report No. 63-2) may be written as follows:

$$N^*_\infty(\infty,\Theta,\emptyset) = N^*_\infty(z_t,\Theta',\emptyset') \left[\frac{1 - T_\infty(\infty,\Theta)}{1 - T_\infty(z_t,\Theta')}\right], \qquad (4)$$

where

$N^*_{\infty}(\infty,\theta,\phi)$ is the path radiance of the downward inclined path of sight θ,ϕ from the target to any altitude outside the atmosphere (∞),

$N^*_{\infty}(z_t,\theta',\phi')$ is the path radiance (i.e., the radiance of the sky as seen from the target) of an upward inclined path of sight θ',ϕ' which has the same angle from the sun as does the downward inclined path of sight θ,ϕ,

$T_{\infty}(\infty,\theta)$ is the beam transmittance of the downward inclined path of sight θ,ϕ from the target to any altitude outside the atmosphere (∞),

and

$T_{\infty}(z_t,\theta')$ is the beam transmittance of the path θ',ϕ' from space to target.

Data from the solar transmissometer, after air mass correction, provide the two values of beam transmittance required by Eq. (4).

The radiance of the sky as seen from the target along the upward inclined path of sight θ',ϕ' can easily be measured by means of a telephotometer stationed at the target. It should be noted that ordinarily there are a number of skyward directions for which the path of sight has the same angle from the sun as does the downward inclined path of sight from ground to space. Data for any of these paths may be used in Eq. (4) and should produce the same value of

$N^*_{\infty}(\infty,\theta,\phi)$. Ordinarily the calculation is made for several such acceptable upward inclined paths as an insurance against an unrecognized abnormality (e.g., an unnoticed wisp of cloud) in one of the selected directions.

If the sky contains scattered or broken clouds the measurement of sky radiance must be made in the clear portions of the sky only. If no appropriate clear region of the sky can be found, the method cannot be used. Such a condition prevailed during the flight of the photographic aircraft on 16 August 1962 so that no path radiance values could be found for that occasion. On all of the ten flights which followed, however, cloud interference did not prevent path radiance values from being obtained. Experience with the technique described by this report has not yet been sufficient to estimate the probability of occurrence of conditions when cloud interference prohibits the method from being applied on occasions when the cloud cover is sufficiently broken to permit observations from space along nearly vertical paths of sight to be made at reasonably frequent intervals.

Measurements from Ground Stations

In summary, a solar transmissometer and an appropriate telephotometer can be used at the ground to measure all of the transmittance and radiance values called for by Eqs. (1) and (4). In so doing the telephotometer is used to measure the inherent radiance of the background as viewed along the downward inclined path of sight θ,ϕ and to measure the radiance of the sky in one or more selected upward inclined paths

of sight θ', ϕ'. Insertion of these measured values in Eqs. (4) and (1) enable the contrast transmittance applicable to any target to be calculated. For convenience Eqs. (1) and (4) have been combined and the result written

$$ {}_b\tau_\infty(\infty,\theta,\phi) \equiv \frac{C_\infty(\infty,\theta,\phi)}{C_o(z_t,\theta,\phi)} = $$

$$ = \frac{{}_bN_o(z_t,\theta,\phi)\ T_\infty(\infty,\theta)}{{}_bN_o(z_t,\theta,\phi)\ T_\infty(\infty,\theta) + N^*_\infty(z_t,\theta',\phi')\left[\dfrac{1 - T_\infty(\infty,\theta)}{1 - T_\infty(z_t,\theta')}\right]} . \qquad (5) $$

It will be noted that the form of the right-hand member of Eq. (5) is such that if the same telephotometer is used for the measurement of the inherent radiance of the background and the radiance of the sky, any error in absolute calibration of this instrument will have no effect on the magnitude of the contrast transmittance ${}_b\tau_\infty(\infty,\theta,\phi)$. If separate instruments are used, utmost care must be exercised to insure that they read the same radiometric quantity in the same absolute units; this instrumental equivalence is frequently difficult to achieve. A weakness in the experiments described in this report is that quite different photometric instrumentation was used in the measurement of ${}_bN_o(z_t,\theta,\phi)$ and $N^*_\infty(z_t,\theta',\phi')$.

3. INSTRUMENTATION

Throughout the years 1955 to 1959 the Visibility Laboratory conducted joint ground-based and airborne experiments in atmospheric optics under a cooperative program between the Air Force Cambridge Research Laboratories and the U. S. Navy's Bureau of Ships. An instrumented B-29 Air Force aircraft performed the airborne experiments and an instrumented Navy trailer van provided the ground station facility. After the B-29 aircraft was decommissioned in 1959, occasional experiments were conducted with the trailer van alone, and it was available for use at Wright-Patterson Air Force Base during the summer of 1962 when the data described by this report were obtained. With the approval of the Bureau of Ships, the trailer was taken over the road from San Diego to Wright-Patterson Air Force Base during May of 1962. From that time until the experiments covered by this report began on 16 August 1962, the trailer was in position alongside the Reconnaissance Laboratory targets at Wright Field. Rehearsals, calibrations, and adjustments were carried out prior to the beginning of the series of data flights on 16 August. Copies of three documentary photographs showing the trailer in its position beside the Reconnaissance Laboratory's targets were supplied by the Air Force for inclusion in this report as Figs. 1, 2, and 3. The caption of Fig. 3 is in error: the control van is on the left and the geophysical van (the Visibility Laboratory van) is on the right. In this photograph and in Fig. 2, the sky-scanning telephotometer can be seen atop a

FIG 1

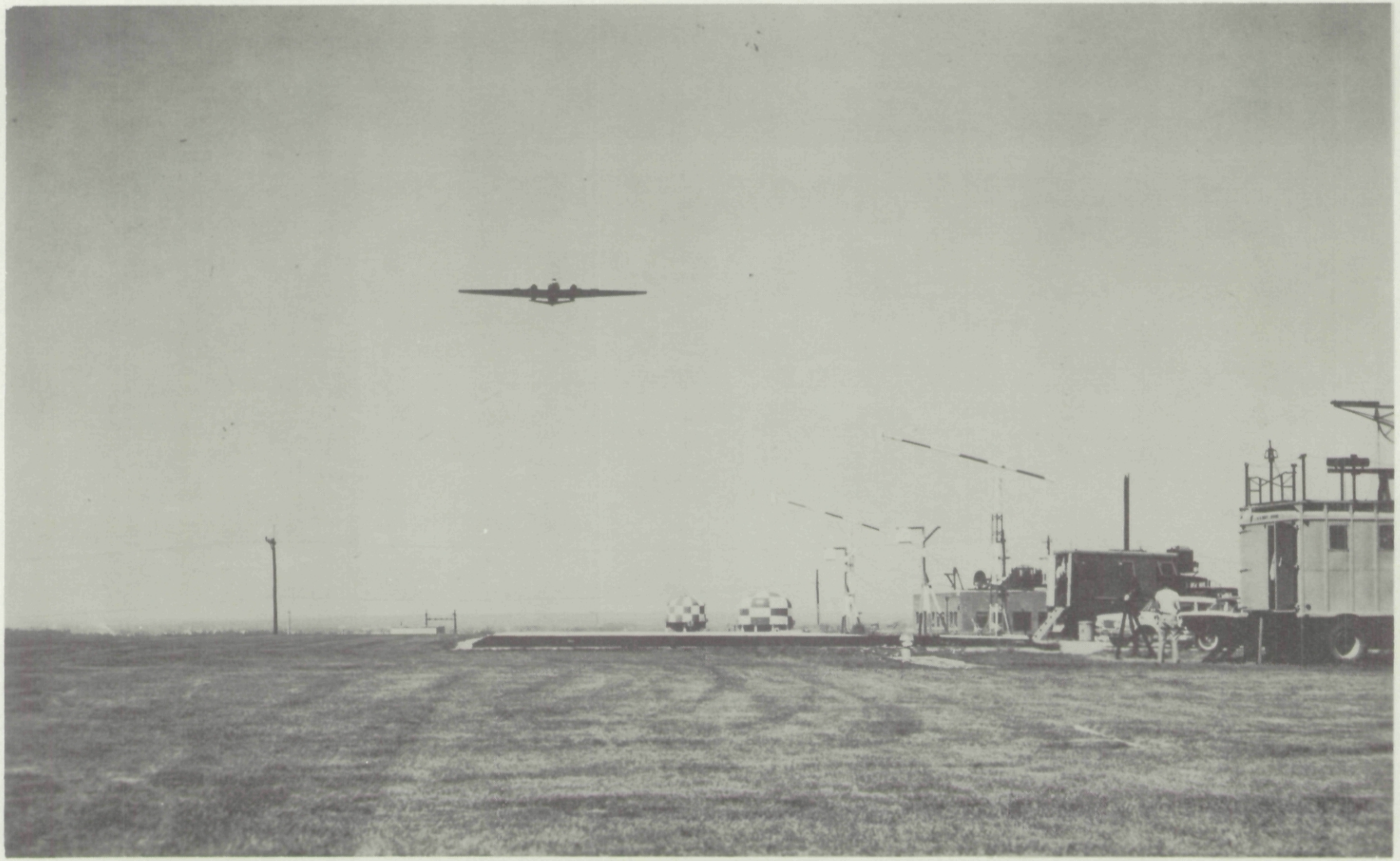

PHOTOGRAPHIC CONTRAST REDUCTION EXPERIMENT
AIRCRAFT APPROACHING TARGETS

ASD
ASTDP

DATE: 22 AUG 62
NEG. NR.. 62-2300

FIG 2

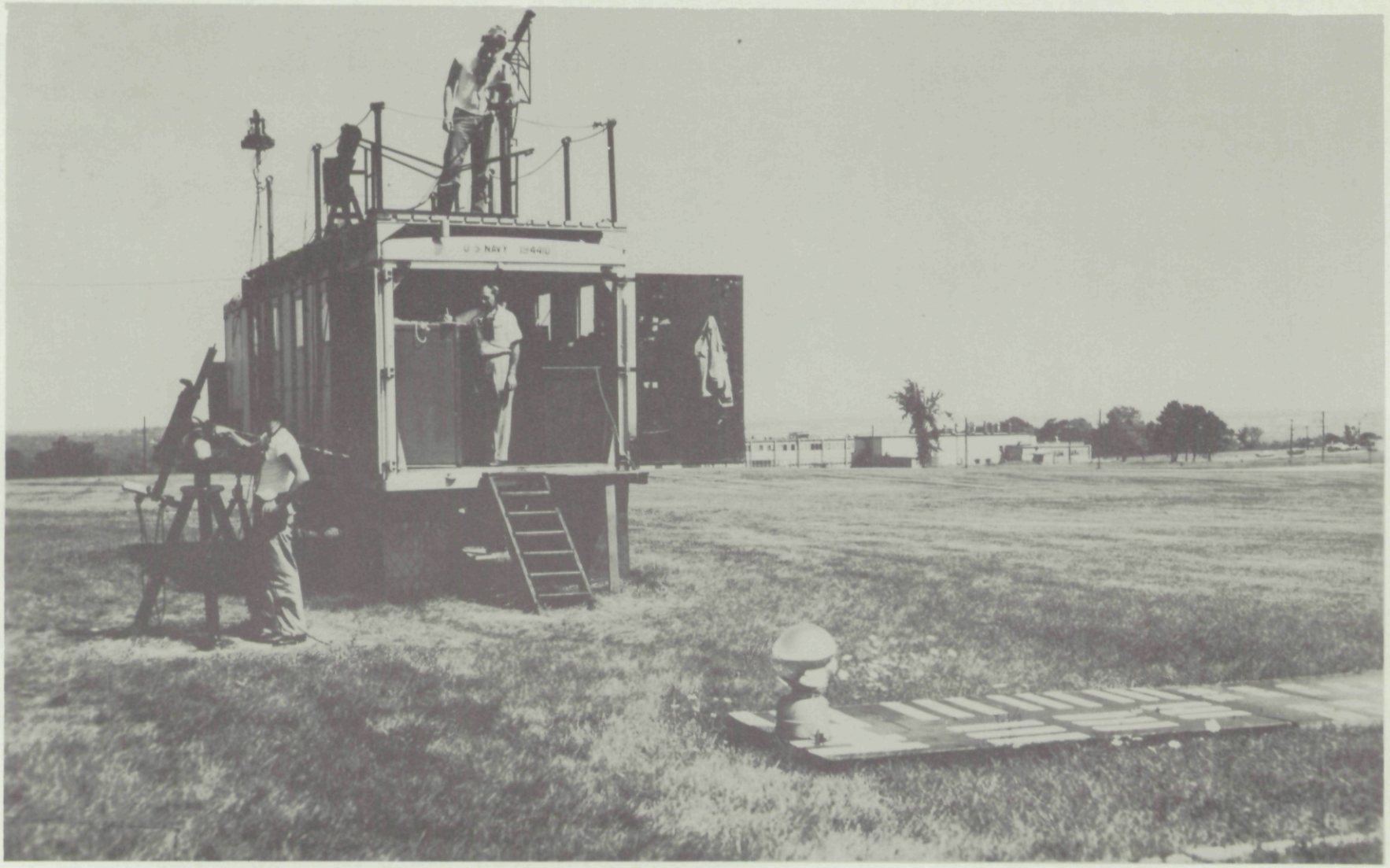

PHOTOGRAPHIC CONTRAST REDUCTION EXPERIMENT
GEOPHYSICAL DATA COLLECTION VAN

ASD
ASTDP

DATE: 22 AUG 62
NEG. NR. 62-2301

FIG 3

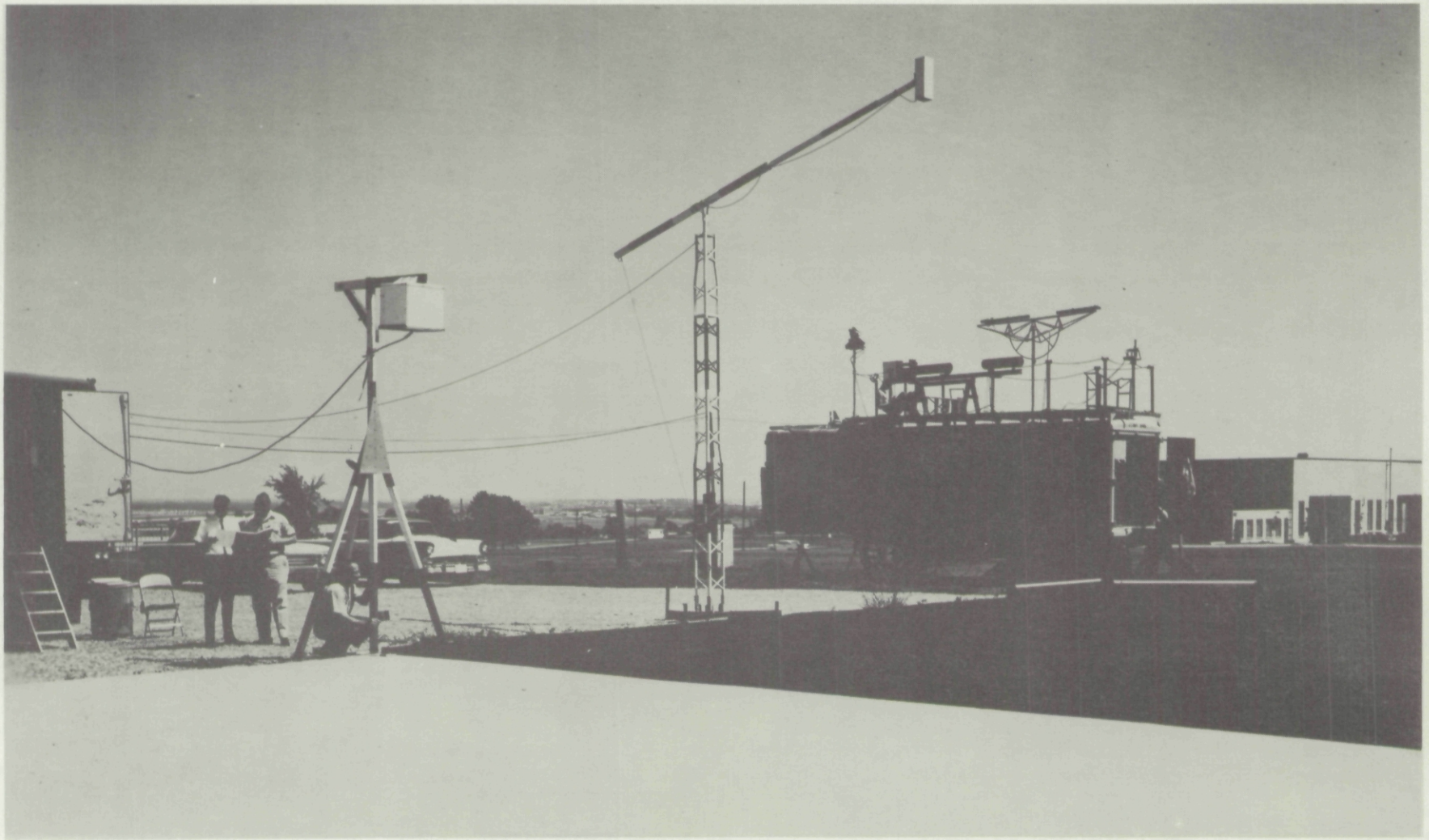

PHOTOGRAPHIC CONTRAST REDUCTION EXPERIMENT
GEOPHYSICAL VAN (LEFT) AND CONTROL VAN (RIGHT)

ASD
ASTDP

DATE: 22 AUG 62
NEG. NR. 62-2304

pole located at the extreme left end of the platform on top of the van. The solar transmissometer is supported by a tripod located on the ground near the opposite end of the van. Other sensor equipments can be seen on the van-top platform, but they were not used in the experiments described by this report.

The solar transmissometer is also pictured and described in Fig. 1 of the Appendix.

The Sky-Scanning Telephotometer

Figure 4 of this report depicts the sky-scanning telephotometer, which can be seen in Figs. 2 and 3, on an elevated mounting atop a short pole on the roof platform of the trailer. The telephotometer consisted of a telescope constructed from half of a 7 x 50 binocular to which an RCA 931A multiplier phototube and a filter-changing mechanism has been attached at the eyepiece and a sunshade added to the objective mounting. This assembly was carried by a motor-driven trunnion and turret so constructed that it provided an automatic sweep of the entire sky. In operation the telescope rotated automatically about a horizontal axis from the horizon upward through the zenith and over to the opposite horizon. In this position the turret automatically rotated about a vertical axis through an azimuth angle of 10°. Thereafter the telescope rotated once more from its horizontal position upward through the zenith and over to the opposite horizontal position.

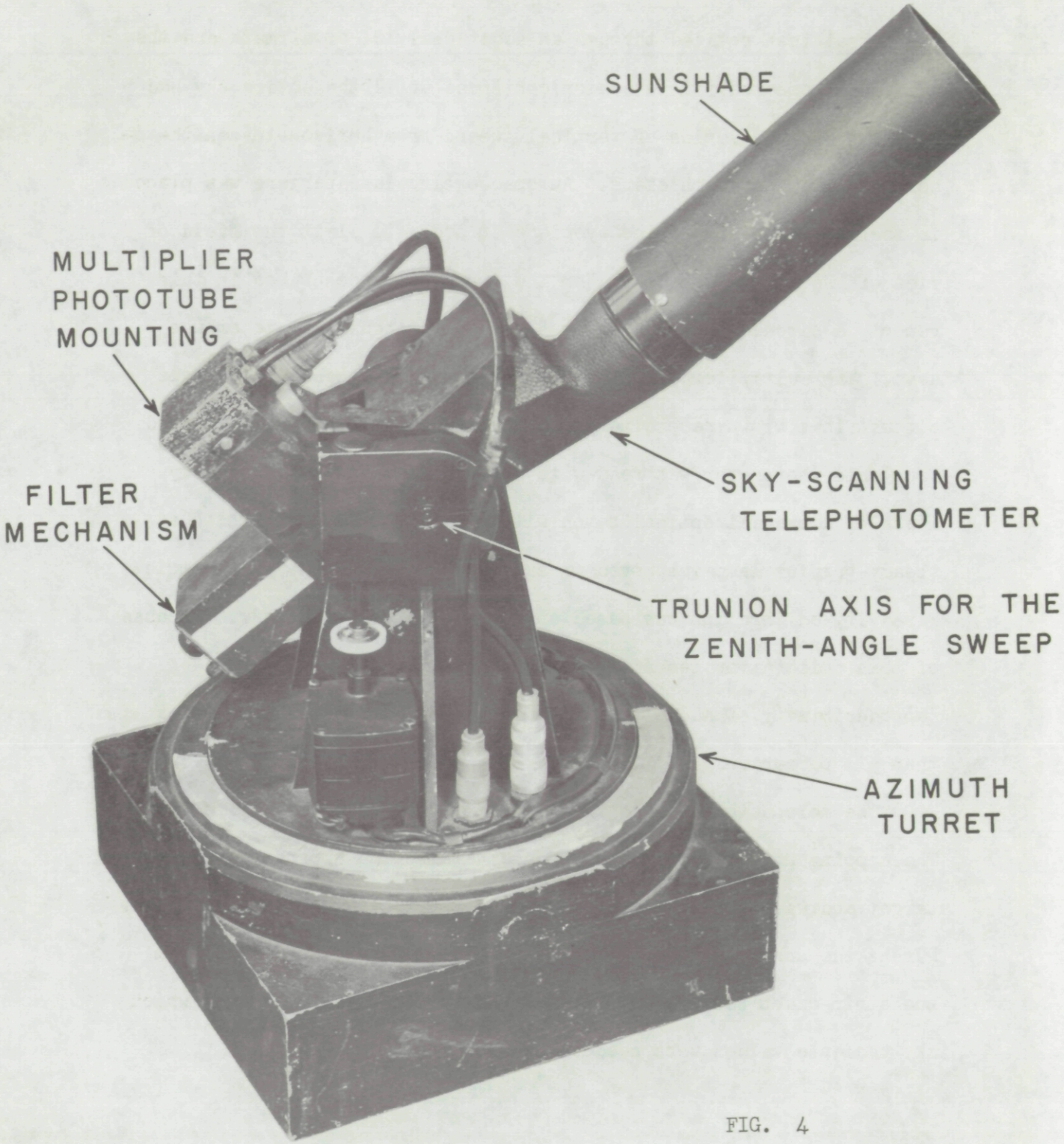
SUNSHADE
MULTIPLIER PHOTOTUBE MOUNTING
FILTER MECHANISM
SKY-SCANNING TELEPHOTOMETER
TRUNION AXIS FOR THE ZENITH-ANGLE SWEEP
AZIMUTH TURRET

FIG. 4

The turret then rotated through an additional 10° of azimuth and the sweep was repeated. This action continued until the entire sky had been mapped by a series of vertical sweeps from horizon-to-zenith-to-horizon in 10° azimuth steps. An opaque circular aperture was placed in the reticle plane of the eyepiece in order to limit the field of view of the telephotometer. For the experiments described in this report, a circular field of view 5° in total angular diameter was used. The multiplier phototube was connected through a Sweet-type circuit to a Brown recording potentiometer. The strip-chart record from this photometer was read with a calibration rule obtained by means of a special optical bench within the trailer along which a steady-burning lamp was moved in such a manner that the photometric linearity calibration was based upon the inverse square law. Because of this calibration technique, the photometric linearity and reproducibility of all of the photoelectric photometers was better than $\pm$ 1 percent.

The telephotometer required six minutes to map the entire sky. The mapping procedure was started as the airplane approached the target and was completed soon after the airplane had passed overhead. During the subsequent reduction of the data, points were read from the strip-chart record only for those paths of sight θ', ϕ' for which sky radiance values were needed for use in Eqs. (4) and (5).

Spectral Sensitivity

Prior to the departure of the trailer from San Diego, the Reconnaissance Laboratory supplied data on the spectral sensitivity of the aerial camera carried by the airplane in order that the Visibility Laboratory could filter its photoelectric photometers to match the aerial camera. The photographic spectral sensitivity was stated to represent Panatomic X aerial film used with a Wratten No. 58 green filter. Figure 5 is a comparison between the photographic spectral sensitivity specified by the Reconnaissance Laboratory and the measured spectral sensitivity of the photoelectric equipment used by the Visibility Laboratory.

All of the sky radiance data obtained under Contract AF 33(657)-7739 were obtained with a green filter and Visibility Laboratory 931A multiplier phototube No. 295. The green filter consisted of six layers of Wratten gelatins as follows: 1 thickness of Wratten No. 61 filter; 2 thicknesses of Wratten No. 2B filter; 1 thickness Wratten 2.0 neutral density filter; 1 thickness Wratten 0.5 neutral density filter; 1 thickness Wratten 0.2 neutral density filter. See Fig. 5 for the measured spectral sensitivity of this phototube-filter combination.

Duplicate phototube-filter sets were used for the solar transmissometer, and the spectral sensitivity depicted by Fig. 5 can be considered as applicable to that instrument also.

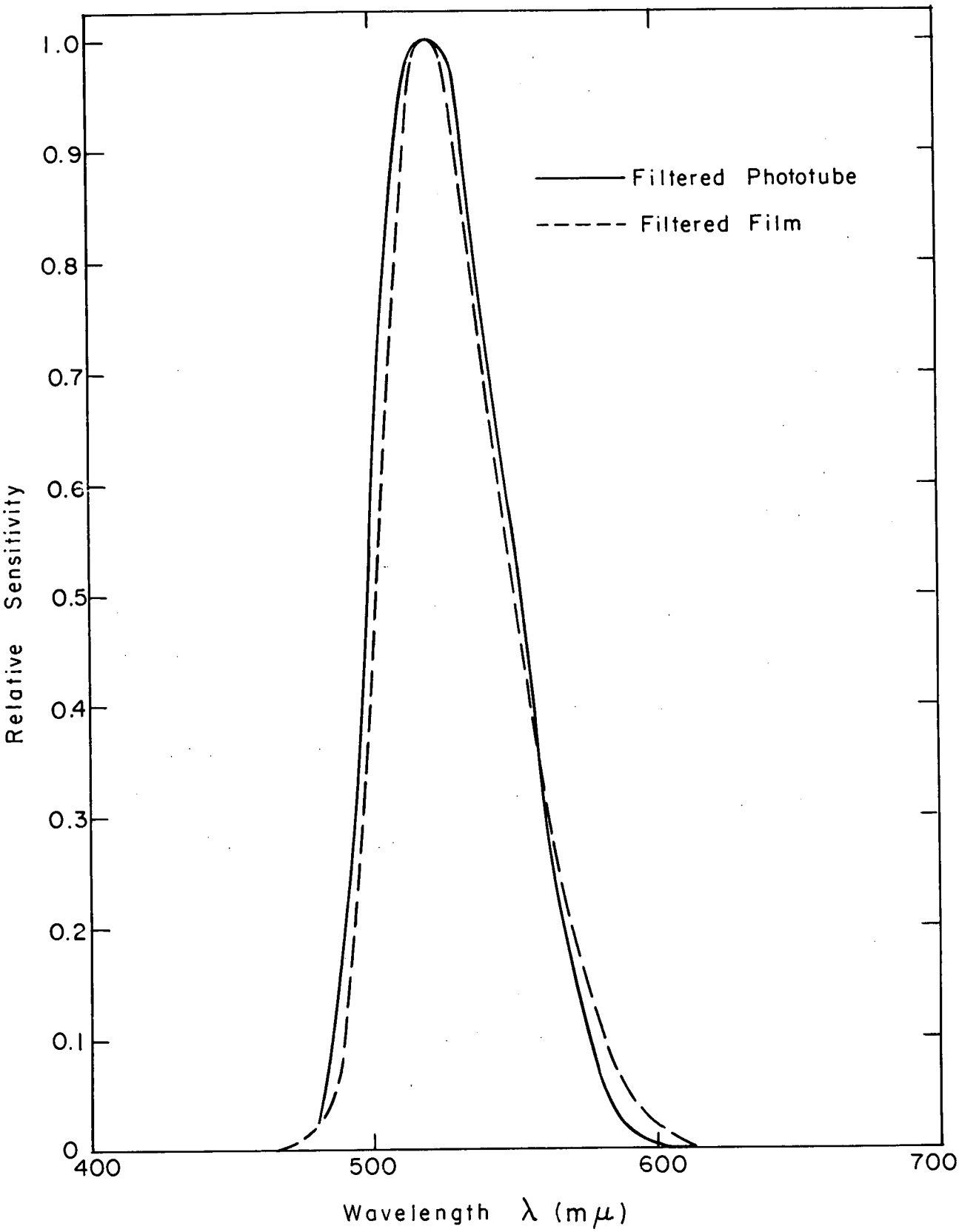
1.0
0.9
0.8
0.7
0.6
0.5
0.4
0.3
0.2
0.1
0
Relative Sensitivity
Filtered Phototube
Filtered Film
400
500
600
700
Wavelength λ (mμ)

Figure 5

Background Radiance

The inherent radiance of the background terrain was not measured directly. Instead, values of terrain reflectance and target reflectances were obtained by Cornell University by means of photographic photometry on the ground and from the aerial photographs produced by the Reconnaissance Laboratory airplane. These reflectances were combined with ground irradiance data measured by means of the Visibility Laboratory's photoelectric irradiance photometer depicted by Fig. 6. This simple device consisted of a 931A multiplier phototube covered by a filter wheel and surmounted by a vertical tube at the top of which was a translucent, white, plastic disk carefully prepared and tested for "cosine response" so that the reading of the photometer was strictly proportional to the radiant power per unit of area impinging on the flat, horizontal upward-facing surface of the translucent disk. The spectral sensitivity of the irradiance photometer was closely identical with that of the sky-scanning telephotometer and the solar transmissometer.

Radiometric Calibration

All three of the photoelectric sensors were carefully calibrated to read in the same absolute units. Incandescent radiometric standard lamps derived from the National Bureau of Standards were used as the basis for these calibrations. As in the case of the other instruments, the irradiance photometer was connected by a Sweet-type circuit to a Brown recording potentiometer. The readings of all three of the

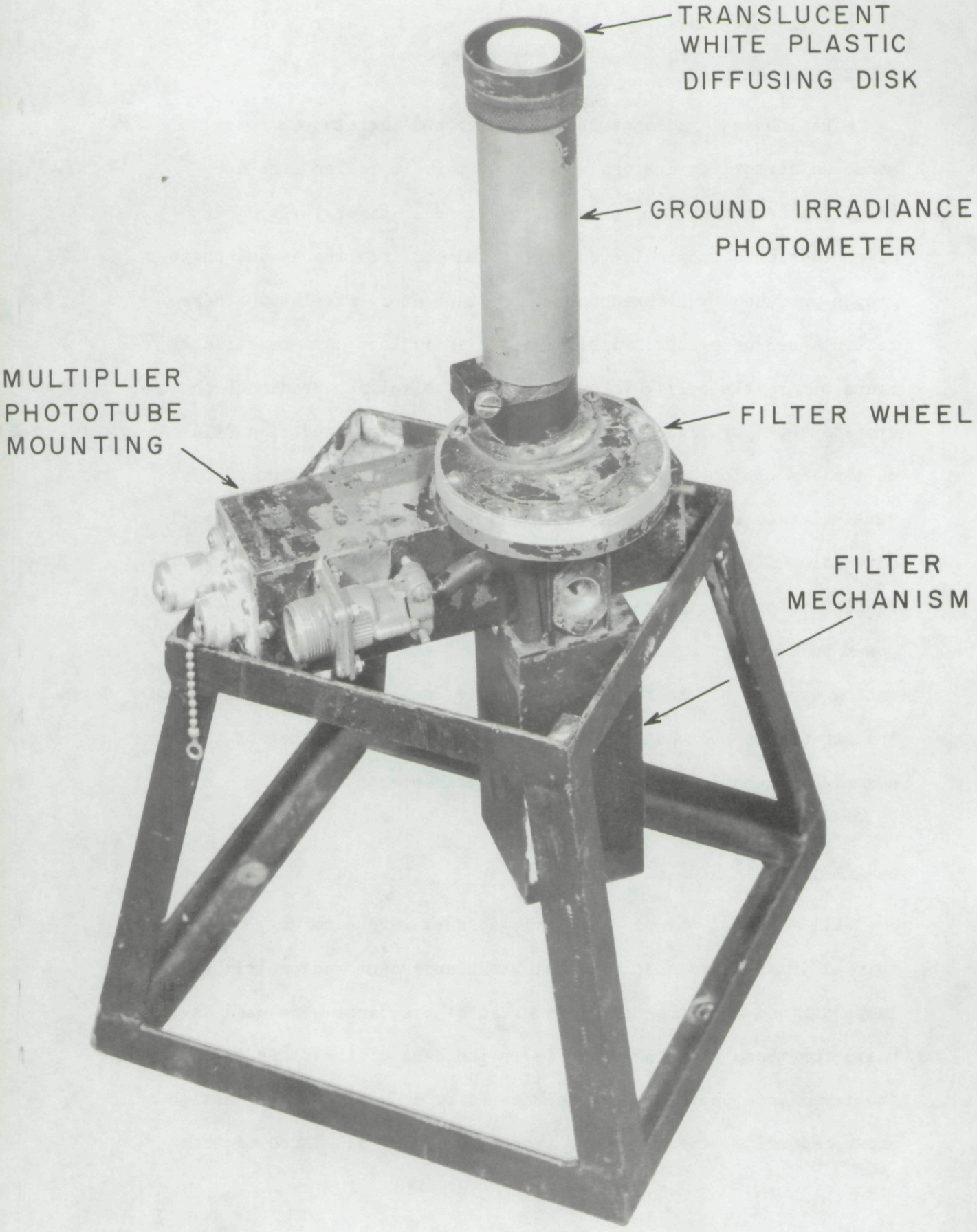
TRANSLUCENT
WHITE PLASTIC
DIFFUSING DISK
GROUND IRRADIANCE
PHOTOMETER
MULTIPLIER
PHOTOTUBE
MOUNTING
FILTER WHEEL
FILTER
MECHANISM

FIG. 6

photoelectric photometers were recorded simultaneously on strip-chart recorders inside the trailer, and these readings were coordinated by radio with the passage of the aircraft over the target.

4. RESULTS

As provided by University of California Proposal No. UCSD 990 and subsequently by Air Force Contract AF 33(657)-7739, the goals of the Visibility Laboratory experiments were values of beam transmittance, path radiance, and contrast transmittance for vertical target-to-space paths of sight. Tables and graphs beginning on page 31 at the end of this report present these results.

Beam Transmittance and Path Radiance

In the tables which follow, the values of beam transmittance for the target-to-space vertical path derived from solar transmissometer data are given, and predicted values of path radiance for the same target-to-space vertical path as derived by means of Eq. (4) from beam transmittance and sky radiance data are listed for each of ten flights at the particular times when the aircraft photographed the targets. Preflight and postflight data of the same type are also given. Despite the fact that all of the occasions covered by these tables represent "clear" days, a considerable variation in beam transmittance and path radiance are evidenced by the data obtained in Tables I through XI and corresponding Figs. 7 through 17, which

show the same information in graphical form.

Contrast Transmittance

Tables I through XI also give values of ground irradiance as measured by the photoelectric irradiance meter depicted by Fig. 6. These data, when combined with reflectance of the terrain or of any background against which a target may be seen, can be used to calculate the values of inherent background radiance which are required in Eq. (5) in order to evaluate the contrast transmittance of downward vertical paths of sight. Since a nearly limitless number of target background luminances are possible, a nearly limitless number of contrast transmittances can be calculated. In each case, however, the contrast transmittance thus calculated applies to every target or target complex which may appear against the selected background.

Frequently targets and confusion objects are located on terrain having a reasonably uniform reflectance. In this case the background for the target and the surround of the target-background complex are the same. This special case is of unique and fundamental interest because the path radiance is always partially dependent on the inherent radiance of the terrain surrounding the target-background complex; in fact, contrast transmittance referred to terrain reflectance is sometimes called the contrast transmittance for the path of sight because it is, generally speaking, that contrast datum of greatest utility in connection with most target detection and

recognition problems.

Tables I through XI contain three columns of contrast transmittance values corresponding with three backgrounds; namely, terrain reflectance, the reflectance of the black target used by the Reconnaissance Laboratory, and the reflectance of the white target used for the aerial photography. Although the three sets of numbers are widely different, each is applicable to any target which could appear against the specified background. All three values of contrast transmittance would be altered if the terrain had a different reflectance.

Perturbations Due to the Background

In the case of the contrast transmittances for the white and for the black backgrounds, respectively, it is assumed that the white or black background areas are so small that their presence imposes no appreciable perturbation on the path radiance. A worthwhile extension of the 1962 experimental program might be a study of background perturbation on path radiance and contrast transmittance. Such a study should evolve rules-of-thumb not presently available by means of which the limiting background areas for a given terrain and background combination could be estimated and an approximate path radiance correction indicated for backgrounds greater in area than the perturbation-free limit.

5. SPECIAL FORMS OF CONTRAST TRANSMITTANCE

The preceding discussion has been concerned with contrasts and contrast transmittances of the universal type, i.e., those which apply to any target. Experience from many fields and with a wide gamut of practical detection and recognition problems shows that this form of contrast is of maximum utility and generality. In certain instances, however, special forms of contrast, each having its own defining relation and equations, have a real or an apparent advantage for some particular problem. A considerable number of specially defined contrasts have been used in previous Visibility Laboratory papers, books, and reports. Names such as absolute contrast, sequential contrast, edge contrast, equilibrium contrast, time-averaged contrast, resolution contrast, chromatic contrast, equivalent achromatic contrast, and contrast ratio are among those that have been used in special cases. Preliminary results from aerial photographic experiments on the flight of 7 September 1962 have recently been received from Cornell Aeronautical Laboratory expressed in a specialized form of contrast known here as bar resolution contrast, ${}_{ij}\overline{\overline{C}}_r(z,\theta,\phi)$, defined in Visibility Laboratory notation as

$$ {}_{ij}\overline{\overline{C}}_r(z,\theta,\phi) = \frac{{}_iN_r(z,\theta,\phi) - {}_jN_r(z,\theta,\phi)}{{}_iN_r(z,\theta,\phi) + {}_jN_r(z,\theta,\phi)} = - {}_{ji}\overline{\overline{C}}_r(z,\theta,\phi) \, . \qquad (6) $$

This is one of a family of specialized resolution contrast quantities which include point resolution contrast ${}_{ij}\ddot{C}_r(z,\theta,\phi)$, and sine resolu-

tion contrast ${}_{ij}\tilde{C}_r(z,\theta,\phi)$. These specialized forms of resolution contrast are non-universal; that is to say, they apply to only one target-background combination and cannot be used for any other target that may appear against the specified background. The use of such a highly restricted form of contrast is convenient, obviously, only in some special circumstance. Bar resolution contrasts, for example, have been widely used by television engineers, since bar resolution targets are commonly used and have special significance with respect to the raster scan employed in television systems. Also, the ratio of (peak-to-peak) AC-to-DC signal output is a convenient electrical quantity for use in television circuit design. Bar type resolution targets are also frequently employed in testing the resolution of photographic lenses and, therefore, bar resolution contrasts are attractive data for use in certain types of photographic testing when camera and film imposed limitations on the resolution of bar type test objects are of interest.

Bar resolution contrast has a simple algebraic connection with universal contrast for the same target and background combination; thus,

$$ {}_{ij}\bar{\bar{C}}_r(z,\theta,\phi) = \frac{{}_{ij}C_r(z,\theta,\phi)}{2 + {}_{ij}C_r(z,\theta,\phi)} = - {}_{ji}\bar{\bar{C}}_r(z,\theta,\phi) \ . \qquad (7) $$

Bar resolution contrast can also be calculated from universal contrasts for each bar considered as a background. Thus,

$$ {}_{ij}\bar{\bar{C}}_r(z,\theta,\phi) = \frac{{}_{ij}C_r(z,\theta,\phi)\ {}_{ji}C_r(z,\theta,\phi)}{{}_{ji}C_r(z,\theta,\phi) - {}_{ij}C_r(z,\theta,\phi)} = - {}_{ji}\bar{\bar{C}}_r(z,\theta,\phi). \qquad (8) $$

Bar Resolution Contrast Reduction Factor

For bars of equal width the inherent radiance of the dark and light bars are linearly averaged in deriving expressions for bar resolution contrast reduction factor. When the bar widths in the test pattern are, however, unequal a different formulation is desirable.

Bar resolution contrast reduction factor ${}_{ij}\mathcal{T}_r(z,\theta,\phi)$ can be calculated from universal contrast transmittances by means of the simple relation

$$ {}_{ij}\mathcal{T}_r(z,\theta,\phi) = \frac{{}_{i}\mathcal{T}_r(z,\theta,\phi) + {}_{j}\mathcal{T}_r(z,\theta,\phi) - 2\,{}_{i}\mathcal{T}_r(z,\theta,\phi)\,{}_{j}\mathcal{T}_r(z,\theta,\phi)}{2 - {}_{i}\mathcal{T}_r(z,\theta,\phi) - {}_{j}\mathcal{T}_r(z,\theta,\phi)} . \quad (9) $$

It will be clear from Eq. (9) that information is discarded in the formation of bar resolution contrast reduction factor, for two items of information are combined to yield one item. This loss of information, inherent in many of the specialized forms of contrast, sometimes appears as an advantage in connection with the particular problem for which the specialized definition of contrast is adopted. In some cases, however, the advantage is superficial rather than real, either because it masks physical phenomena in a manner which tends to produce ambiguity in the interpretation of experimental results, or because the specialized contrast reduction data cannot be interpreted in terms of other types of test objects or actual targets.

From a fundamental standpoint, it will be noted from Eq. (1), or from the more basic radiative transfer equations from which it is

derived (see Appendix), that two independent physical properties of the atmosphere are always involved in an image transmission radiative transfer process. They are the beam transmittance and the path radiance. If these two properties of the path are known, then all forms of contrast, contrast transmittance, or contrast reduction factor can be calculated for any pair of objects having known inherent radiances. Thus, any specialized definitions which yield a single number description for the atmospheric path are an incomplete specification applicable only to some special case. Bar resolution contrast, for example, is restricted to a unique pair of objects. Whatever advantage results from the use of bar resolution contrast reduction factor is bought at the expense of a loss in fundamental information concerning the path of sight and, therefore, in the applicability of the data to the imagery of objects other than bar patterns at limiting resolution.

For the sake of comparison with the data being generated by Cornell Aeronautical Laboratory, Tables I through XI include bar resolution contrasts for equal-width black and white bars having the reflectances of the white and black Reconnaissance Laboratory targets.

6. CONCLUSIONS

The primary purpose of the Visibility Laboratory experiments described in this report is that of testing the validity of the proposed new method for predicting ground-to-space beam transmittance,

path radiance, and contrast transmittance from ground station measurements by comparing these predicted values with their ground-to-aircraft counterparts. As of the date of this report, only preliminary data from the aerial photographs made on the morning flight of 7 September 1962 have been reduced by Cornell Aeronautical Laboratory. The bar resolution contrast reduction factor for altitude 50,000 feet on the occasion of this flight reported by Cornell Aeronautical Laboratory is 0.60. The corresponding bar resolution contrast transmittance in the last column of Table IX is 0.80. Beam transmittance and path radiance values for any of the flights have not yet been reported by Cornell. Comparisons and conclusions cannot, therefore, be formed at this time.

30 January 1963

DATA FIGURES AND TABLES

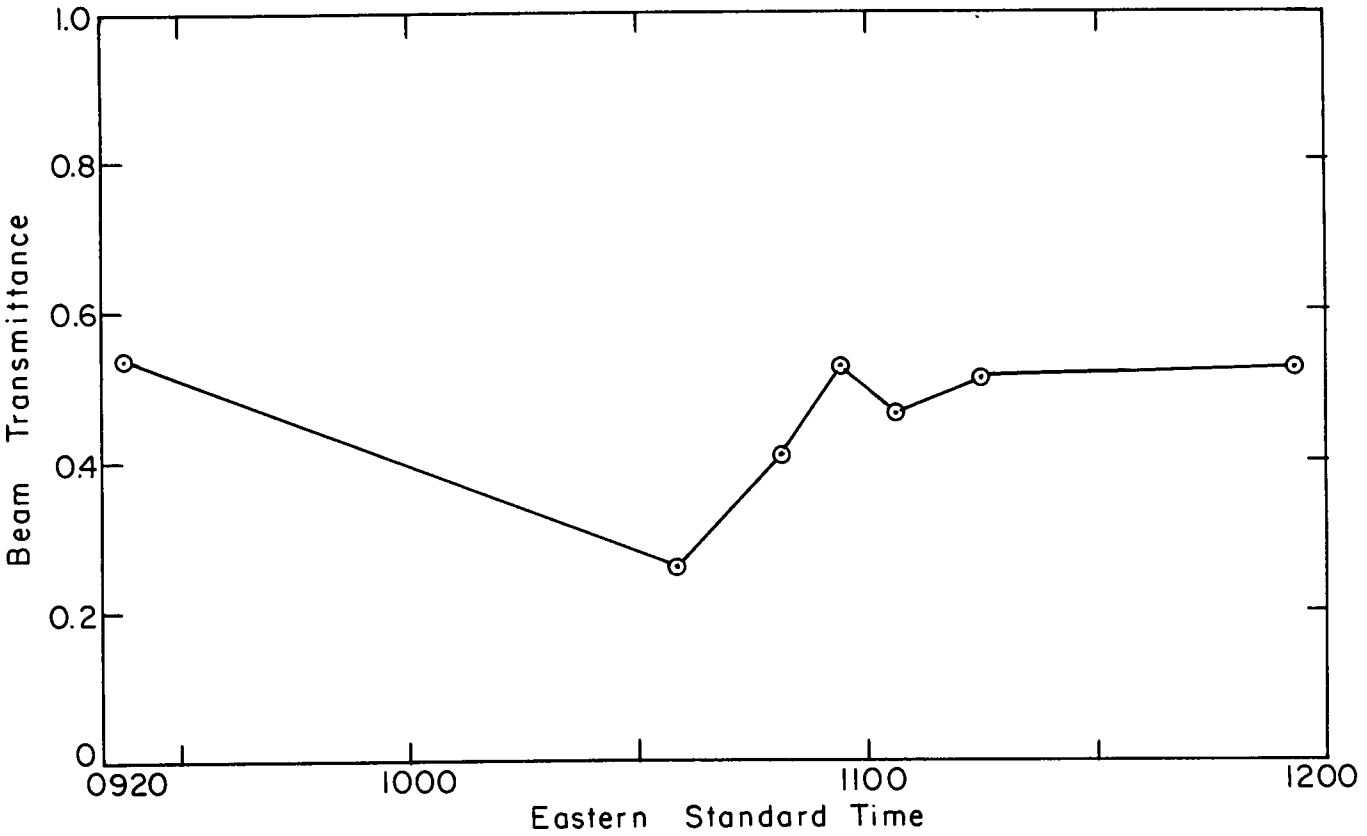

Data of 16 August 1962

Figure 7

TABLE I

DATE OF 16 August 1962

AIRCRAFT ALTITUDE (FEET)	EASTERN STANDARD (TIME)	BEAM TRANSMIT-TANCE	PATH RADIANCE $\left(\frac{\text{WATTS}}{\text{FT}^2}\right)$	IRRADIANCE $\left(\frac{\text{WATTS}}{\text{FT}^2}\right)$	CONTRAST TRANSMITTANCE			BAR RESOLUTION CONTRAST TRANSMITTANCE 0.801 and 0.005
					TERRAIN BACKGROUND REFLECTANCE OF 0.0625 *	WHITE BACKGROUND REFLECTANCE OF 0.801	BLACK BACKGROUND REFLECTANCE OF 0.005	
PREFLIGHT	0923	0.534		4.16				
23 400								
35 500	1035	0.259		3.42				
42 500	1049	0.408		4.45				
50 000	1057	0.522		5.48				
42 500	1104	0.462		5.05				
35 500	1115	0.510		5.05				
23 400								
POSTFLIGHT	1156	0.527		5.67				

*Weighted arithmetic average of estimates by Cornell Aeronautical Lab. from aerial photographs on basis of atmospheric correction factor from 7 September 1962.

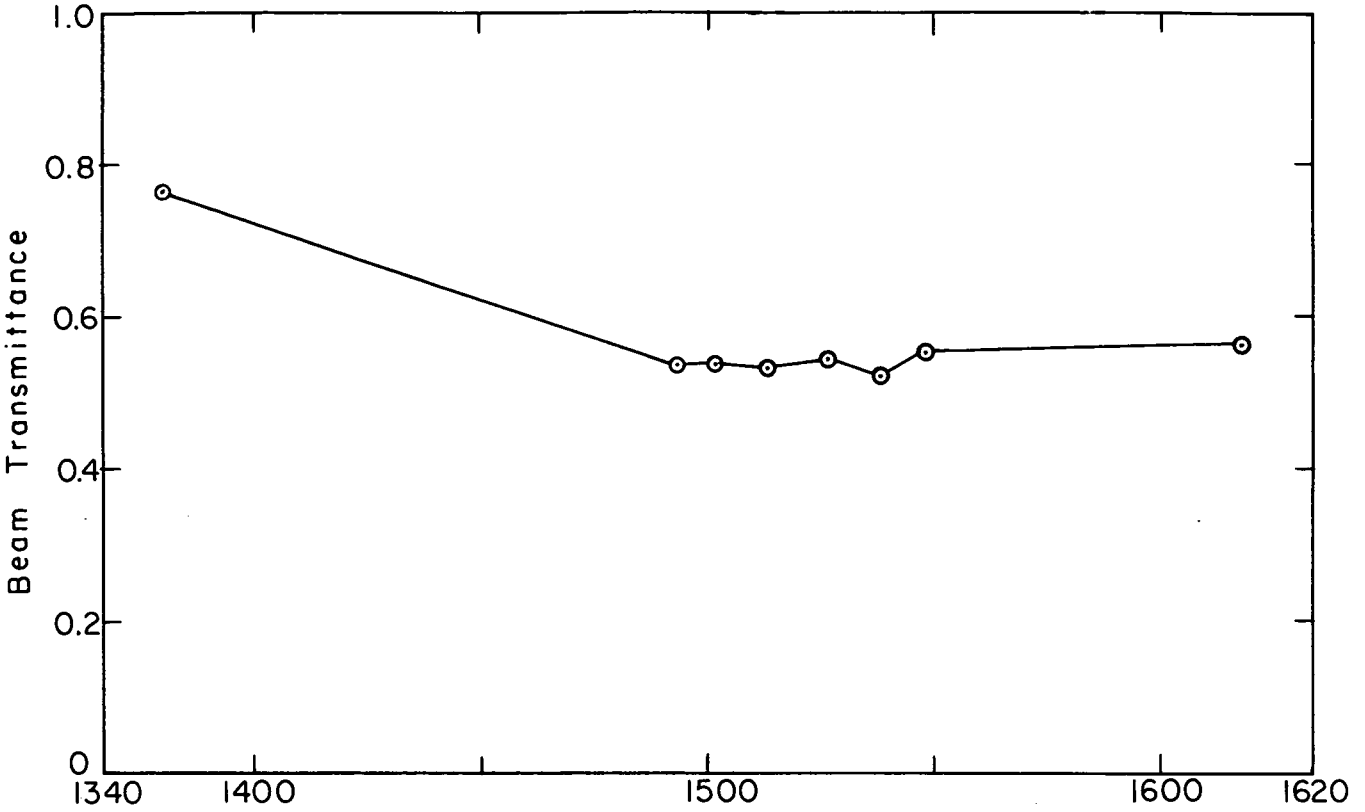

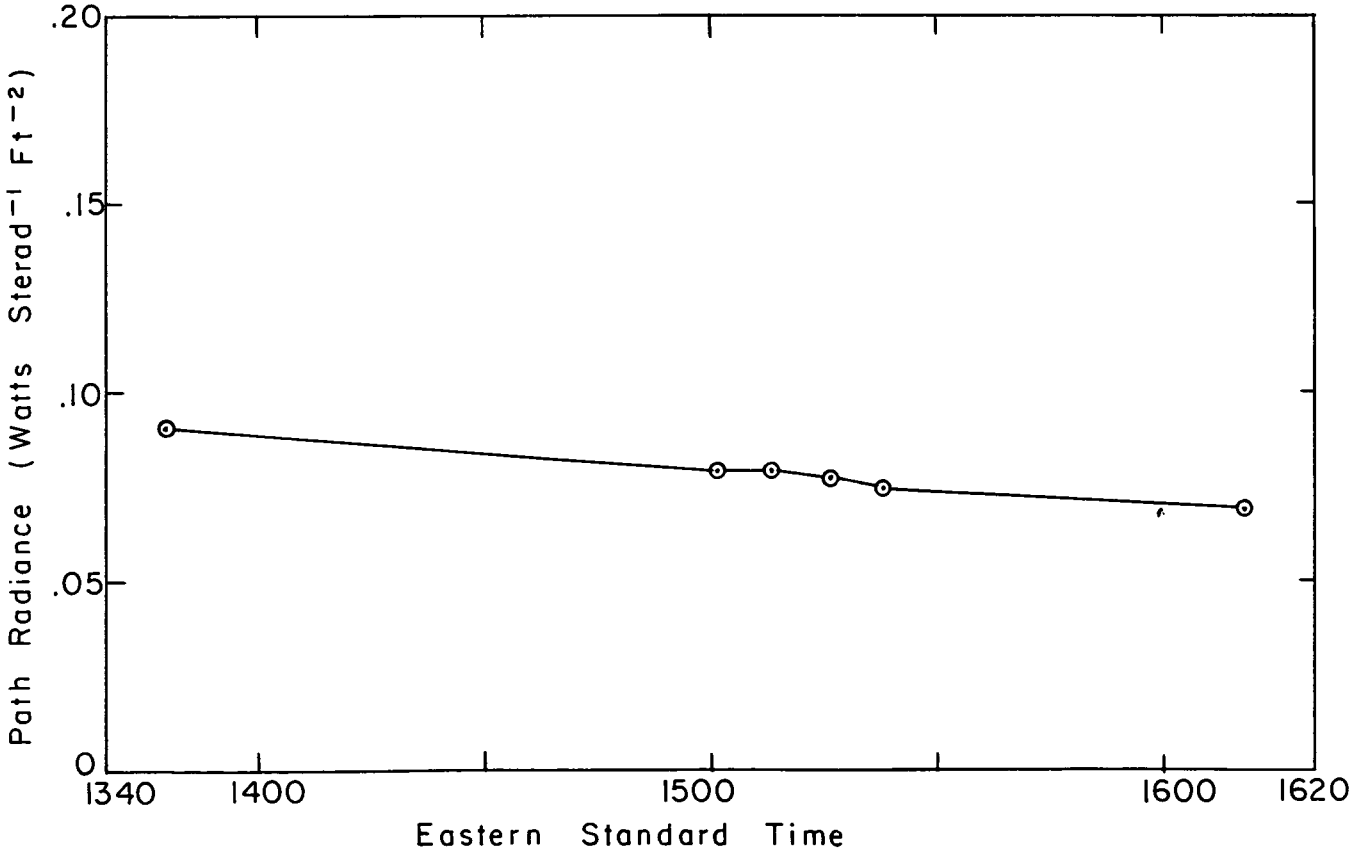

Data of 22 August 1962

Figure 8

TABLE II

DATE OF 22 August 1962

AIRCRAFT ALTITUDE (FEET)	EASTERN STANDARD (TIME)	BEAM TRANSMIT-TANCE	PATH RADIANCE $\left(\frac{\text{WATTS}}{\text{FT}^2}\right)$	IRRADIANCE $\left(\frac{\text{WATTS}}{\text{FT}^2}\right)$	CONTRAST TRANSMITTANCE			BAR RESOLUTION CONTRAST TRANSMITTANCE 0,801 and 0,005
					TERRAIN BACKGROUND REFLECTANCE OF 0.0475 *	WHITE BACKGROUND REFLECTANCE OF 0.801	BLACK BACKGROUND REFLECTANCE OF 0.005	
PREFLIGHT	1348	0.765	0.0912	6.32	0.445	0.931	0.0778	0.871
23 400	1456	0.534		4.66				
35 500	1501	0.538	0.0799	4.66	0.322	0.889	0.0476	0.803
42 500	1508	0.534	0.0797	4.61	0.318	0.887	0.0468	0.798
50 000	1516	0.544	0.0789	4.35	0.312	0.884	0.0455	0.796
42 500	1523	0.528	0.0750	4.30	0.314	0.885	0.0459	0.795
35 500	1529	0.566		4.25				
23 400								
POSTFLIGHT	1611	0.565	0.0693	3.43	0.297	0.877	0.0425	0.783

* Weighted arithmetic average of estimates by Cornell Aeronautical Lab. from aerial photographs on basis of atmospheric correction factor from 7 September 1962.

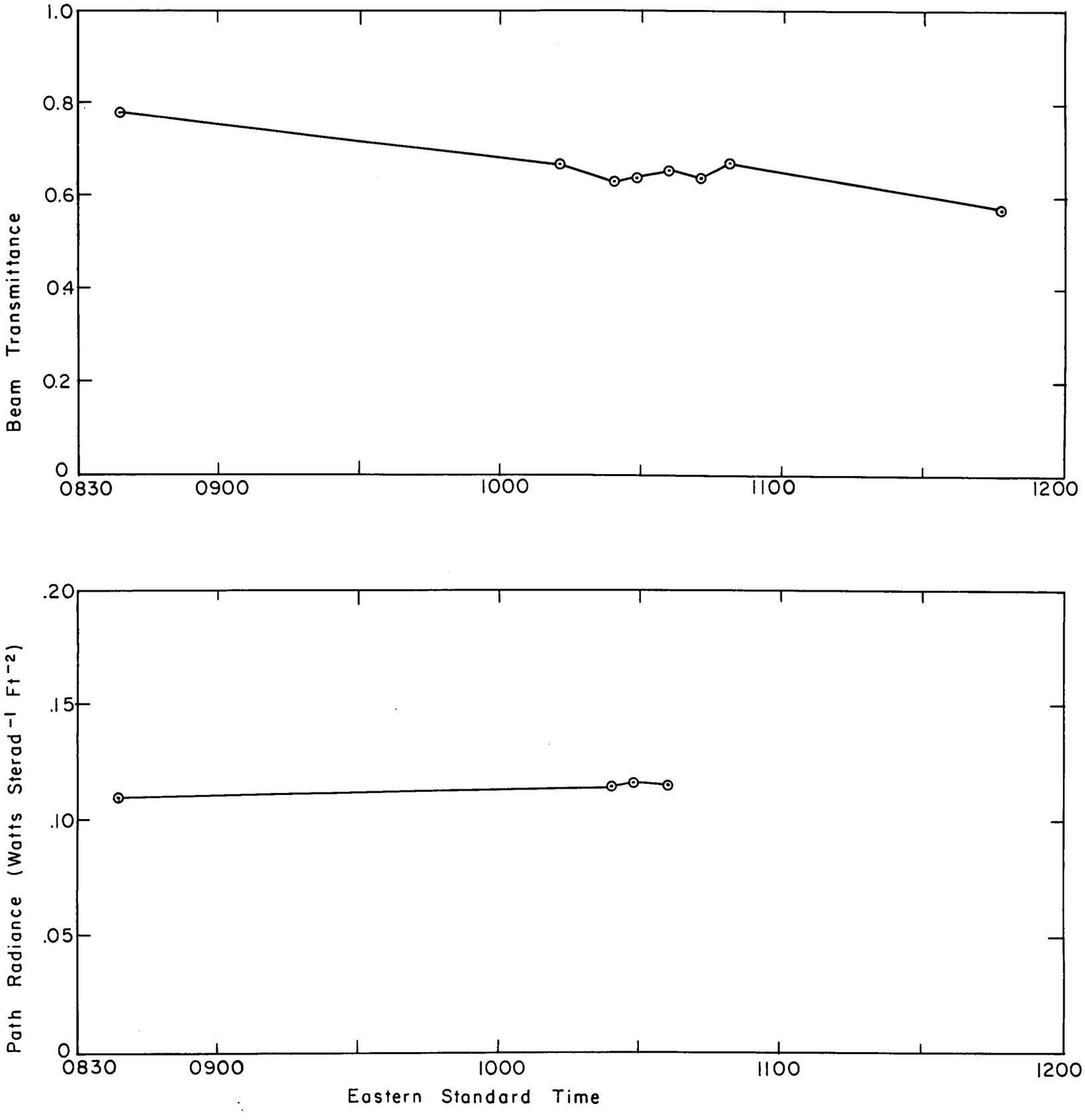

Data of 23 August 1962 (A.M.)

Figure 9

TABLE III

DATE OF 23 August 1962, A.M.

AIRCRAFT ALTITUDE (FEET)	EASTERN STANDARD (TIME)	BEAM TRANSMITTANCE	PATH RADIANCE $\left(\frac{\text{WATTS}}{\text{FT}^2}\right)$	IRRADIANCE $\left(\frac{\text{WATTS}}{\text{FT}^2}\right)$	CONTRAST TRANSMITTANCE			BAR RESOLUTION CONTRAST TRANSMITTANCE 0.801 and 0.005
					TERRAIN BACKGROUND REFLECTANCE OF 0.0650 *	WHITE BACKGROUND REFLECTANCE OF 0.801	BLACK BACKGROUND REFLECTANCE OF 0.005	
PREFLIGHT	0839	0.778	0.110	3.34	0.326	0.858	0.0362	0.752
23 400	1013	0.672		4.50				
35 500	1024.5	0.638	0.115	4.71	0.351	0.869	0.0398	0.770
42 500	1029	0.641	0.117	4.76	0.350	0.869	0.0398	0.770
50 000	1036	0.658	0.116	4.87	0.364	0.876	0.0421	0.780
42 500	1043	0.642		5.05				
35 500	1049	0.672		5.16				
23 400								
POSTFLIGHT	1146	0.572		5.22				

* Weighted arithmetic average of estimates by Cornell Aeronautical Lab. from aerial photographs on basis of atmospheric correction factor from 7 September 1962.

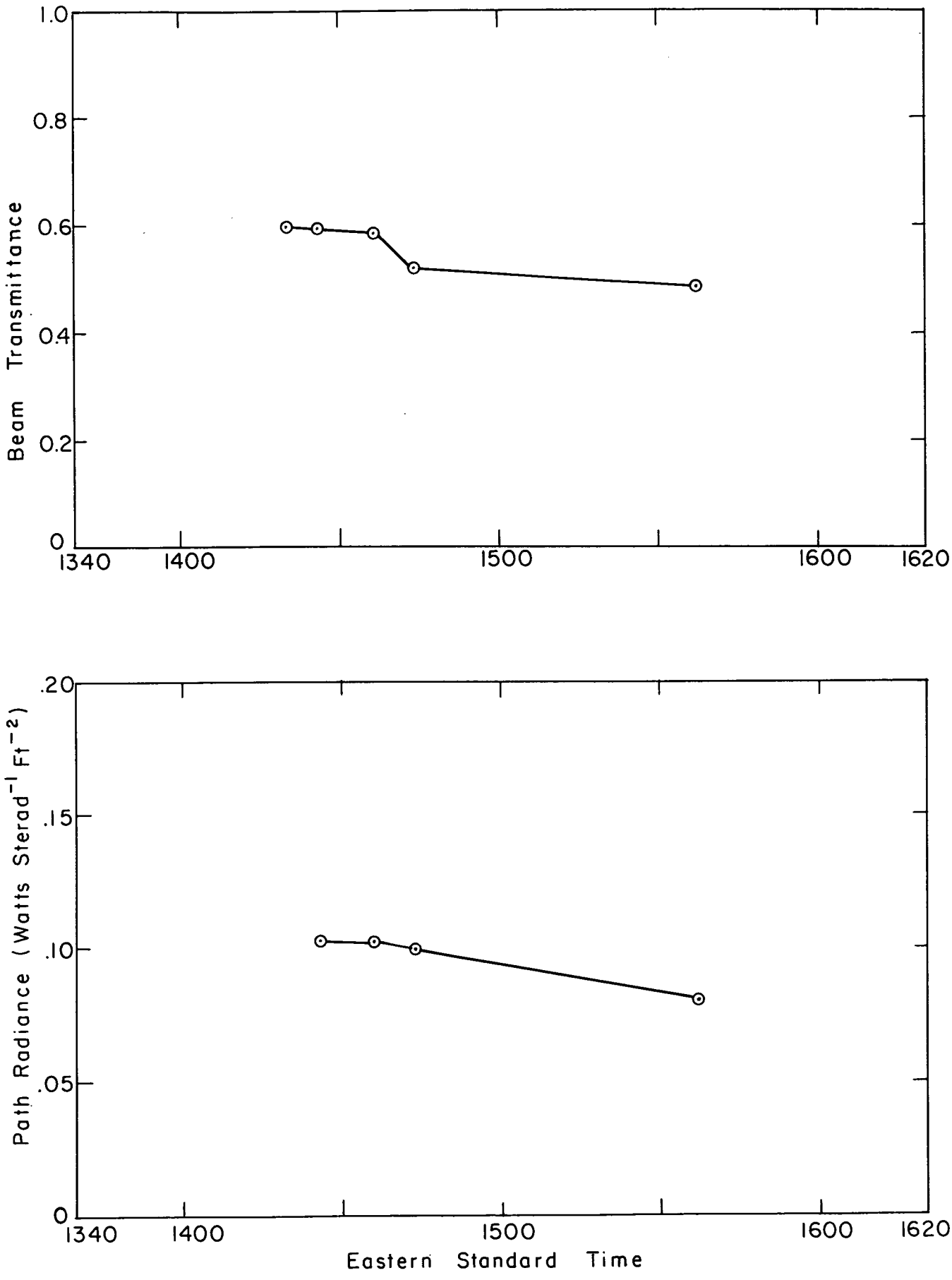

Data of 23 August 1962 (P.M.)

Figure 10

TABLE IV

DATE OF 23 August 1962, P.M.

AIRCRAFT ALTITUDE (FEET)	EASTERN STANDARD (TIME)	BEAM TRANSMIT-TANCE	PATH RADIANCE $\left(\frac{\text{WATTS}}{\text{FT}^2}\right)$	IRRADIANCE $\left(\frac{\text{WATTS}}{\text{FT}^2}\right)$	CONTRAST TRANSMITTANCE			BAR RESOLUTION CONTRAST TRANSMITTANCE 0.801 and 0.005
					TERRAIN BACKGROUND REFLECTANCE OF 0.0565 *	WHITE BACKGROUND REFLECTANCE OF 0.801	BLACK BACKGROUND REFLECTANCE OF 0.005	
PREFLIGHT								
23 400	1420	0.600		5.17				
35 500	1426	0.598	0.103	5.05	0.346	0.882	0.0444	0.789
42 500								
50 000	1436.5	0.587	0.103	4.84	0.332	0.875	0.0419	0.779
42 500								
35 500	1444	0.523	0.100	4.78	0.310	0.864	0.0382	0.762
23 400								
POSTFLIGHT	1537	0.490	0.806	3.97	0.303	0.860	0.0369	0.755

*Weighted arithmetic average of estimates by Cornell Aeronautical Lab. from aerial photographs on basis of atmospheric correction factor from 7 September 1962.

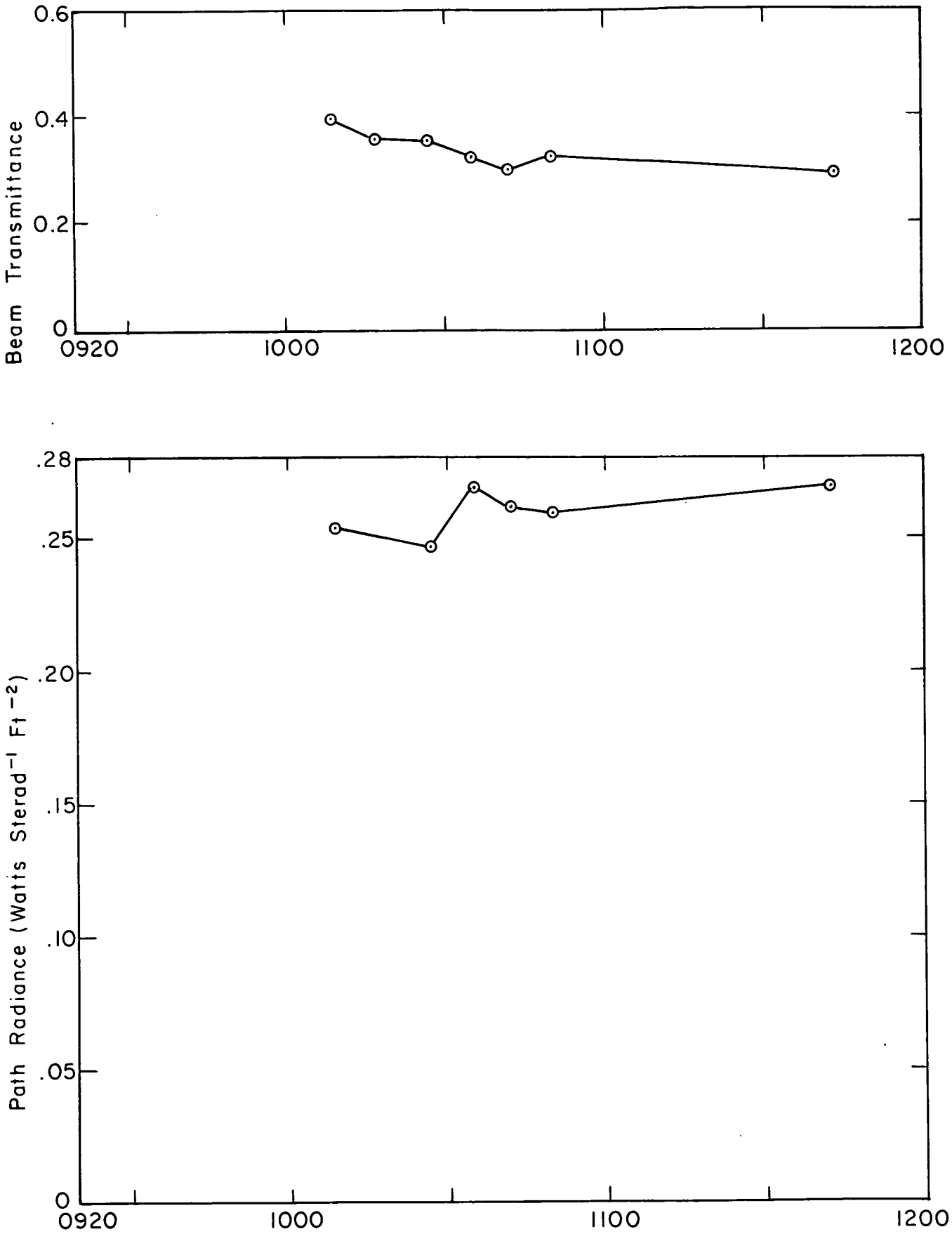

Data of 24 August 1962

Figure 11

TABLE V

DATE OF 24 August 1962

AIRCRAFT ALTITUDE (FEET)	EASTERN STANDARD (TIME)	BEAM TRANSMIT-TANCE	PATH RADIANCE $\left(\frac{\text{WATTS}}{\text{FT}^2}\right)$	IRRADIANCE $\left(\frac{\text{WATTS}}{\text{FT}^2}\right)$	CONTRAST TRANSMITTANCE			BAR RESOLUTION CONTRAST TRANSMITTANCE 0.801 and 0.005
					TERRAIN BACKGROUND REFLECTANCE OF 0.0790 *	WHITE BACKGROUND REFLECTANCE OF 0.801	BLACK BACKGROUND REFLECTANCE OF 0.005	
PREFLIGHT								
23 400								
35 500	1009	0.393	0.254	4.66	0.153	0.648	0.0113	0.481
42 500	1017	0.360		4.51				
	1027	0.351	0.247	4.45	0.137	0.617	0.0100	0.447
50 000	1035	0.322	0.269	4.66	0.123	0.587	0.00882	0.416
42 500	1042	0.300	0.261	4.66	0.119	0.577	0.00844	0.407
35 500	1050	0.326	0.259	4.83	0.132	0.608	0.00954	0.438
23 400								
POSTFLIGHT	1143.5	0.292	0.269	5.28	0.126	0.594	0.00904	0.424

*Weighted arithmetic average of estimates by Cornell Aeronautical Lab. from aerial photographs on basis of atmospheric correction factor from 7 September 1962.

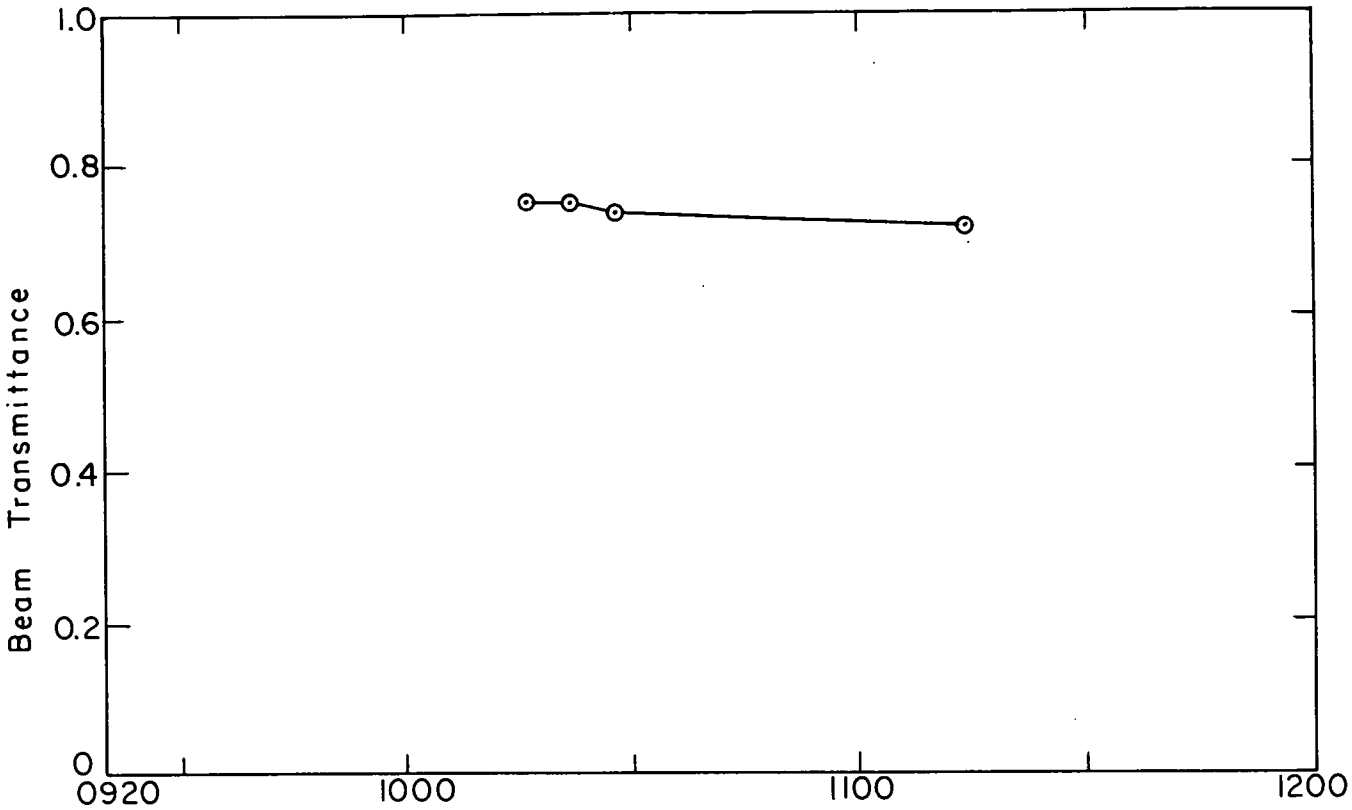
1.0
0.8
0.6
0.4
0.2
0
Beam Transmittance
0920
1000
1100
1200

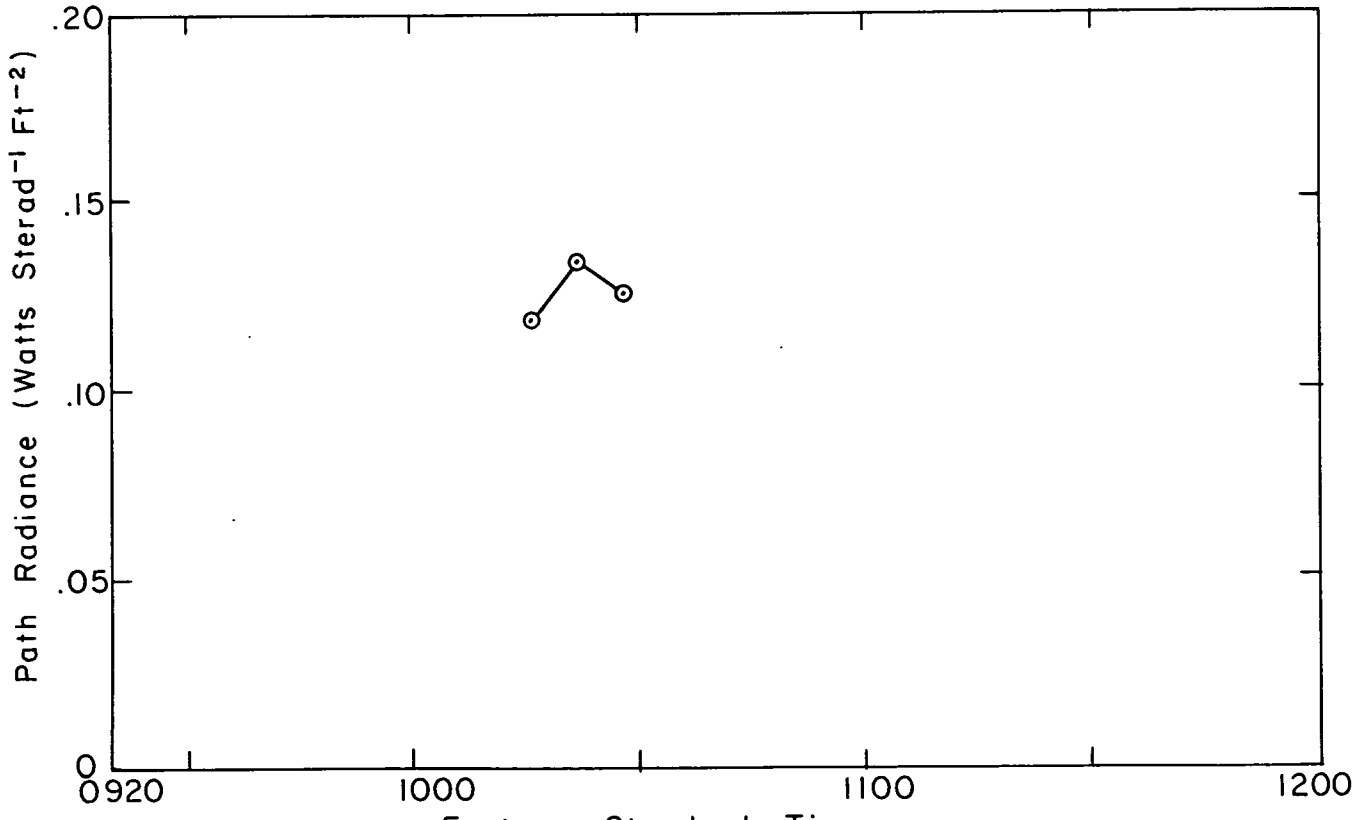
.20
.15
.10
.05
0
Path Radiance (Watts Sterad^{-1} Ft^{-2})
0920
1000
1100
1200
Eastern Standard Time
Data of 27 August 1962

Figure 12

TABLE VI

DATE OF 27 August 1962

AIRCRAFT ALTITUDE (FEET)	EASTERN STANDARD (TIME)	BEAM TRANSMIT-TANCE	PATH RADIANCE $\left(\frac{\text{WATTS}}{\text{FT}^2}\right)$	IRRADIANCE $\left(\frac{\text{WATTS}}{\text{FT}^2}\right)$	CONTRAST TRANSMITTANCE			BAR RESOLUTION CONTRAST TRANSMITTANCE 0.801 and 0.005
					TERRAIN BACKGROUND REFLECTANCE OF 0.0665 *	WHITE BACKGROUND REFLECTANCE OF 0.801	BLACK BACKGROUND REFLECTANCE OF 0.005	
PREFLIGHT								
23 400								
35 500								
42 500	1015.5	0.759	0.119	4.99	0.403	0.815	0.0482	0.798
50 000								
42 500	1022	0.750	0.134	5.29	0.386	0.883	0.0451	0.792
35 500	1028	0.740	0.126	5.35	0.400	0.889	0.0477	0.801
23 400								
POSTFLIGHT	1114	0.721		6.00				

*Weighted arithmetic average of estimates by Cornell Aeronautical Lab. from aerial photographs on basis of atmospheric correction factor from 7 September 1962.

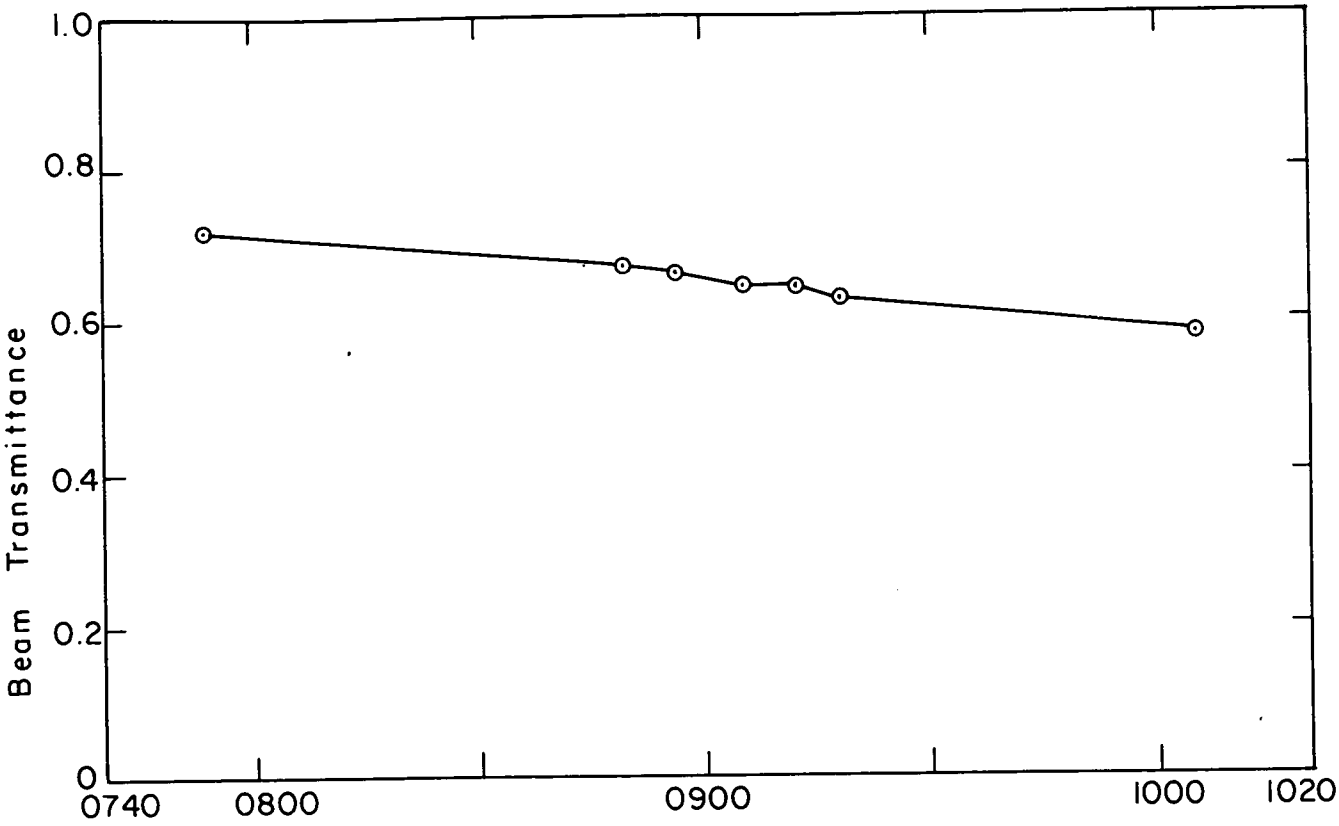

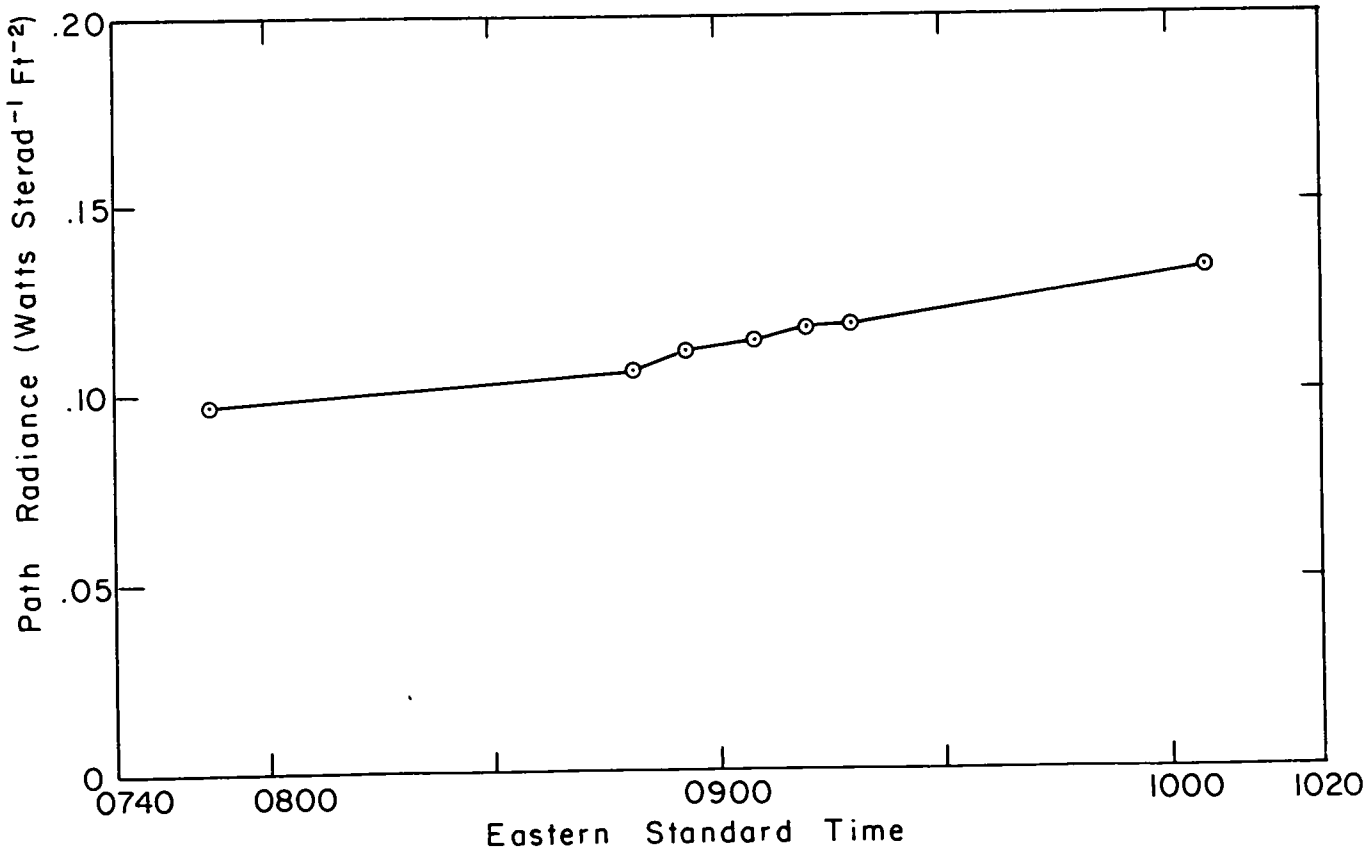

Data of 28 August 1962

Figure 13

TABLE VII

DATE OF 28 August 1962

AIRCRAFT ALTITUDE (FEET)	EASTERN STANDARD (TIME)	BEAM TRANSMITTANCE	PATH RADIANCE $\left(\frac{\text{WATTS}}{\text{FT}^2}\right)$	IRRADIANCE $\left(\frac{\text{WATTS}}{\text{FT}^2}\right)$	CONTRAST TRANSMITTANCE			BAR RESOLUTION CONTRAST TRANSMITTANCE 0.801 and 0.005
					TERRAIN BACKGROUND REFLECTANCE OF 0.0610 *	WHITE BACKGROUND REFLECTANCE OF 0.801	BLACK BACKGROUND REFLECTANCE OF 0.005	
PREFLIGHT	0753.5	0.720	0.0978	2.10	0.231	0.798	0.0240	0.564
23 400								
35 500	0849	0.676	0.106	3.30	0.290	0.843	0.0324	0.730
42 500	0856	0.669	0.111	3.38	0.283	0.839	0.0313	0.723
50 000	0905	0.648	0.114	3.42	0.274	0.832	0.0300	0.714
42 500	0912	0.646	0.117	3.62	0.279	0.836	0.0308	0.719
35 500	0918	0.631	0.118	3.79	0.282	0.838	0.0312	0.722
23 400								
POSTFLIGHT	1005	0.587	0.133	4.32	0.270	0.829	0.0294	0.710

*Weighted arithmetic average of estimates by Cornell Aeronautical Lab. from aerial photographs on basis of atmospheric correction factor from 7 September 1962.

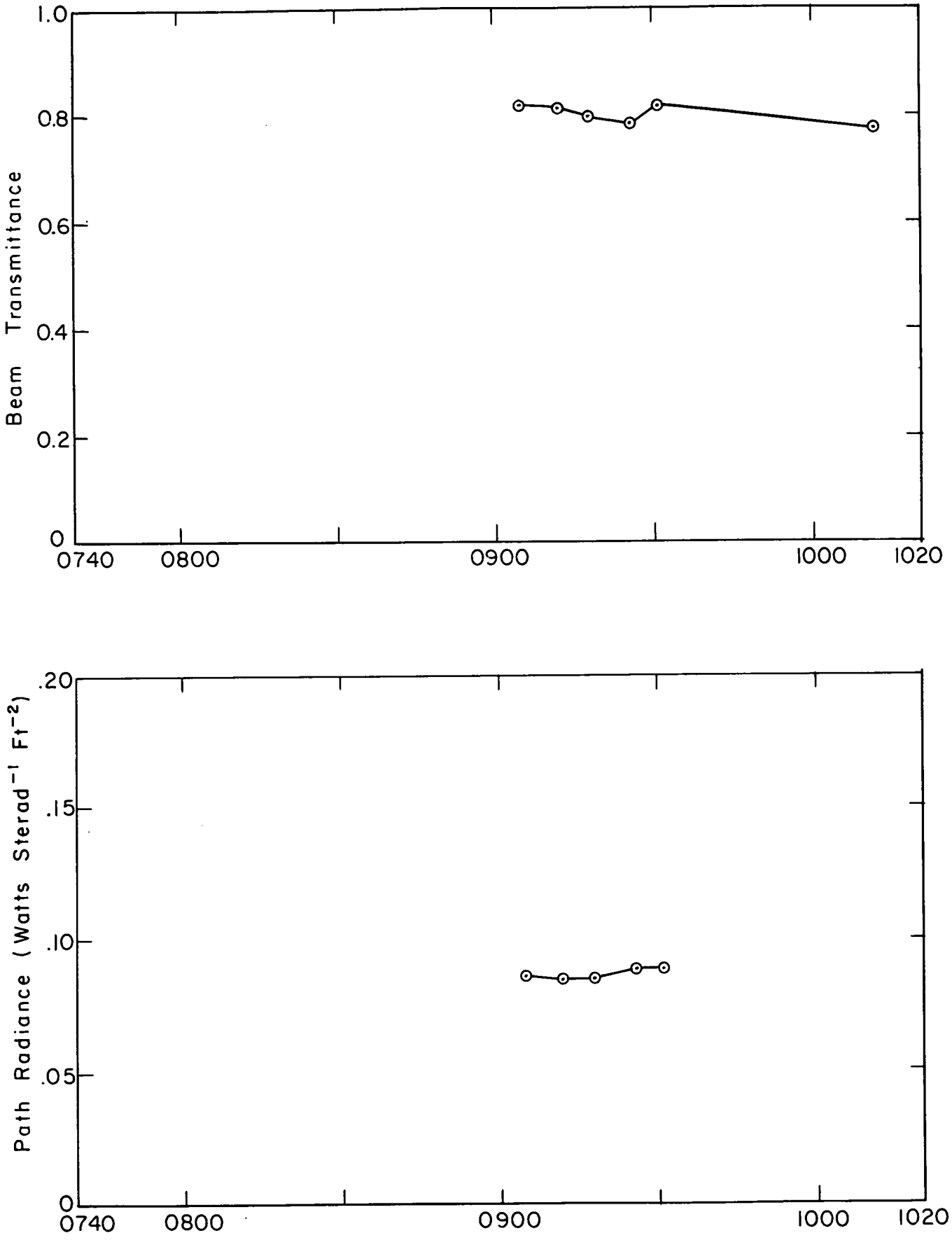

Data of 6 September 1962

Figure 14

TABLE VIII

DATE OF 6 September 1962

AIRCRAFT ALTITUDE (FEET)	EASTERN STANDARD (TIME)	BEAM TRANSMIT-TANCE	PATH RADIANCE $\left(\frac{\text{WATTS}}{\text{FT}^2}\right)$	IRRADIANCE $\left(\frac{\text{WATTS}}{\text{FT}^2}\right)$	CONTRAST TRANSMITTANCE			BAR RESOLUTION CONTRAST TRANSMITTANCE 0.801 and 0.005
					TERRAIN BACKGROUND REFLECTANCE OF 0.0485 *	WHITE BACKGROUND REFLECTANCE OF 0.801	BLACK BACKGROUND REFLECTANCE OF 0.005	
PREFLIGHT								
23 400								
35 500	0905	0.820	0.0860					
42 500	0912	0.817	0.0847	3.96	0.370	0.907	0.0573	0.830
50 000	0918	0.800	0.0846	4.10	0.374	0.908	0.0581	0.832
42 500	0926	0.787	0.0890	4.15	0.361	0.903	0.0551	0.825
35 500	0931	0.818	0.0887	4.35	0.382	0.911	0.0600	0.837
23 400								
POSTFLIGHT	1011.5	0.775		5.73				

*Weighted arithmetic average of estimates by Cornell Aeronautical Lab. from aerial photographs on basis of atmospheric correction factor from 7 September 1962.

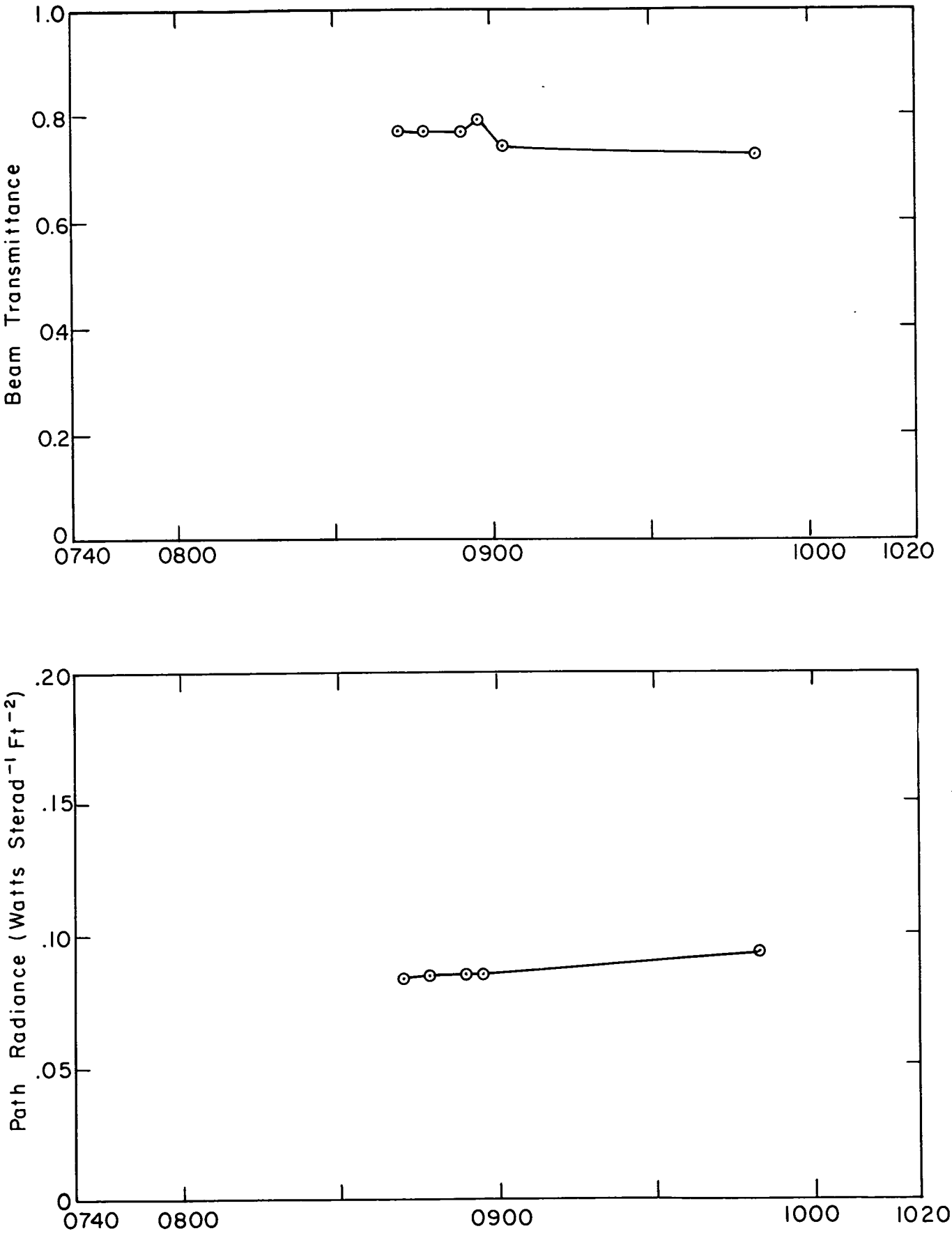
1.0
0.8
0.6
0.4
0.2
0
Beam Transmittance
0740
0800
0900
1000
1020
.20
.15
.10
.05
0
Path Radiance (Watts Sterad^{-1} Ft^{-2})
0740
0800
0900
1000
1020
Eastern Standard Time
Data of 7 September 1962 (A M)

Figure 15

TABLE IX

DATE OF 7 September 1962, A. M.

AIRCRAFT ALTITUDE (FEET)	EASTERN STANDARD (TIME)	BEAM TRANSMIT-TANCE	PATH RADIANCE $\left(\frac{\text{WATTS}}{\text{FT}^2}\right)$	IRRADIANCE $\left(\frac{\text{WATTS}}{\text{FT}^2}\right)$	CONTRAST TRANSMITTANCE			BAR RESOLUTION CONTRAST TRANSMITTANCE 0.801 and 0.005
					TERRAIN BACKGROUND REFLECTANCE OF 0.0808 *	WHITE BACKGROUND REFLECTANCE OF 0.801	BLACK BACKGROUND REFLECTANCE OF 0.005	
PREFLIGHT								
23 400								
35 500	0842	0.779	0.0840	3.24	0.436	0.884	0.0456	0.794
42 500	0847	0.776	0.0853	3.33	0.438	0.885	0.0460	0.796
50 000	0854	0.773	0.0854	3.38	0.440	0.886	0.0463	0.798
42 500	0857	0.793	0.0855	3.45	0.451	0.891	0.0484	0.803
35 500	0902	0.749		3.58				
23 400								
POSTFLIGHT	0950	0.730	0.0926	3.62	0.423	0.879	0.0434	0.785

* Weighted arithmetic average based on measurements by Cornell Aeronautical Lab. of aerial photographs.

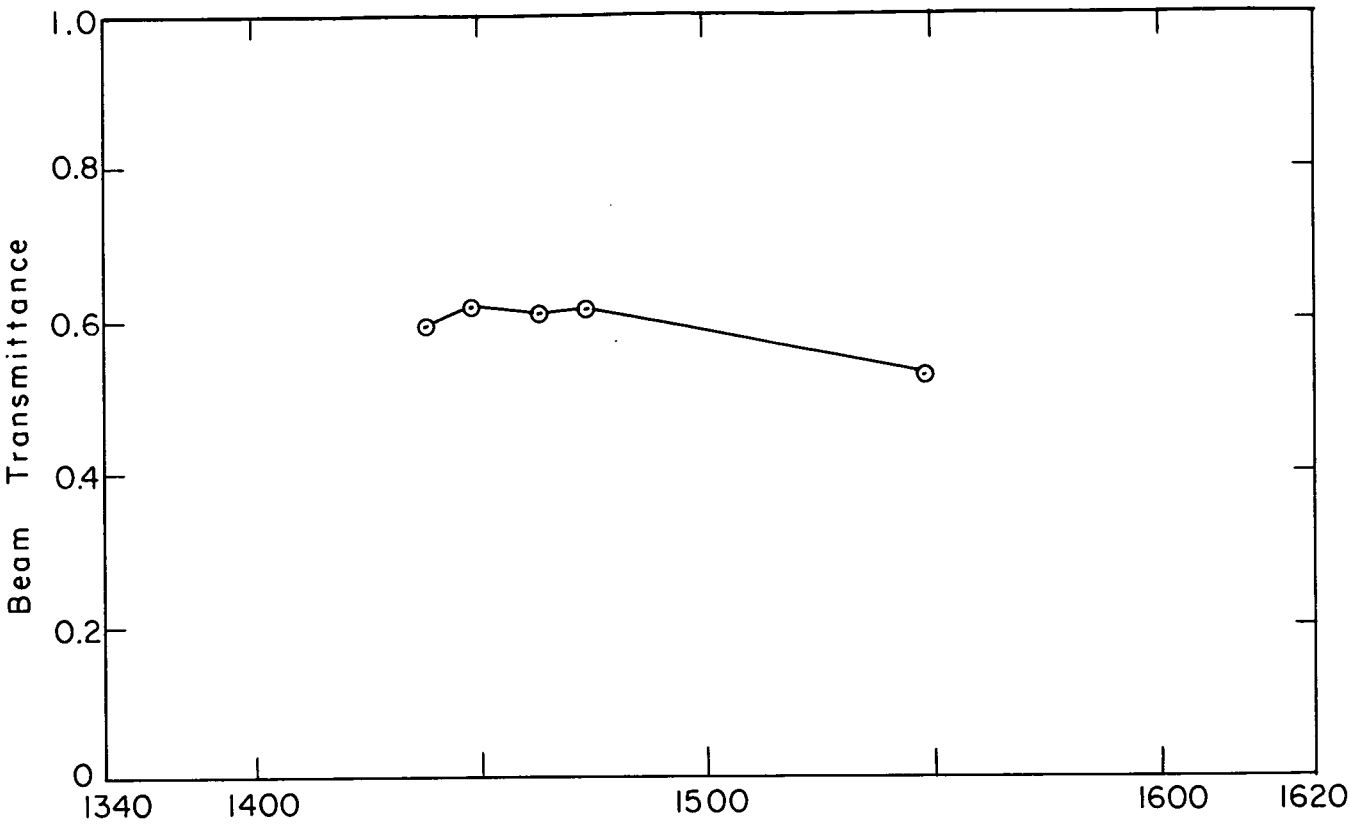

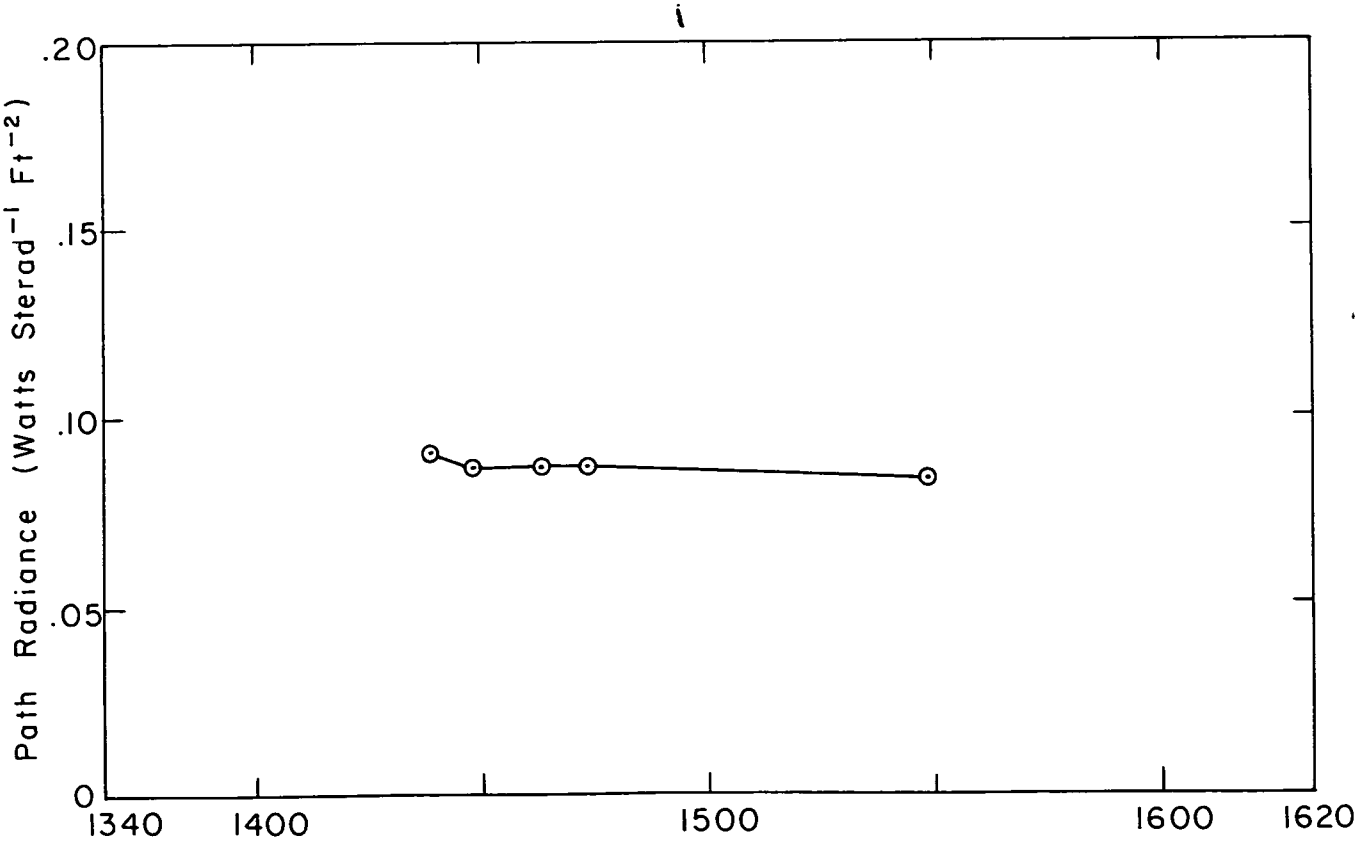

Data of 7 September 1962 (PM)

Figure 16

TABLE X

DATE OF 7 September 1962, P.M.

AIRCRAFT ALTITUDE (FEET)	EASTERN STANDARD (TIME)	BEAM TRANSMIT-TANCE	PATH RADIANCE $\left(\frac{\text{WATTS}}{\text{FT}^2}\right)$	IRRADIANCE $\left(\frac{\text{WATTS}}{\text{FT}^2}\right)$	CONTRAST TRANSMITTANCE			BAR RESOLUTION CONTRAST TRANSMITTANCE 0.801 and 0.005
					TERRAIN BACKGROUND REFLECTANCE OF 0.0339 *	WHITE BACKGROUND REFLECTANCE OF 0.801	BLACK BACKGROUND REFLECTANCE OF 0.005	
PREFLIGHT								
23 400								
35 500	1423	0.595	0.0905	5.27	0.273	0.898	0.0523	0.815
42 500	1429	0.620	0.0872	5.14	0.283	0.903	0.0549	0.825
50 000	1438	0.610	0.0872	5.01	0.275	0.899	0.0528	0.818
42 500	1444	0.616	0.0872	5.08	0.279	0.901	0.0540	0.820
35 500								
23 400								
POSTFLIGHT	1529	0.531	0.0833	4.10	0.220	0.869	0.0399	0.769

*Weighted arithmetic average based on measurements by Cornell Aeronautical Lab. of aerial photographs.

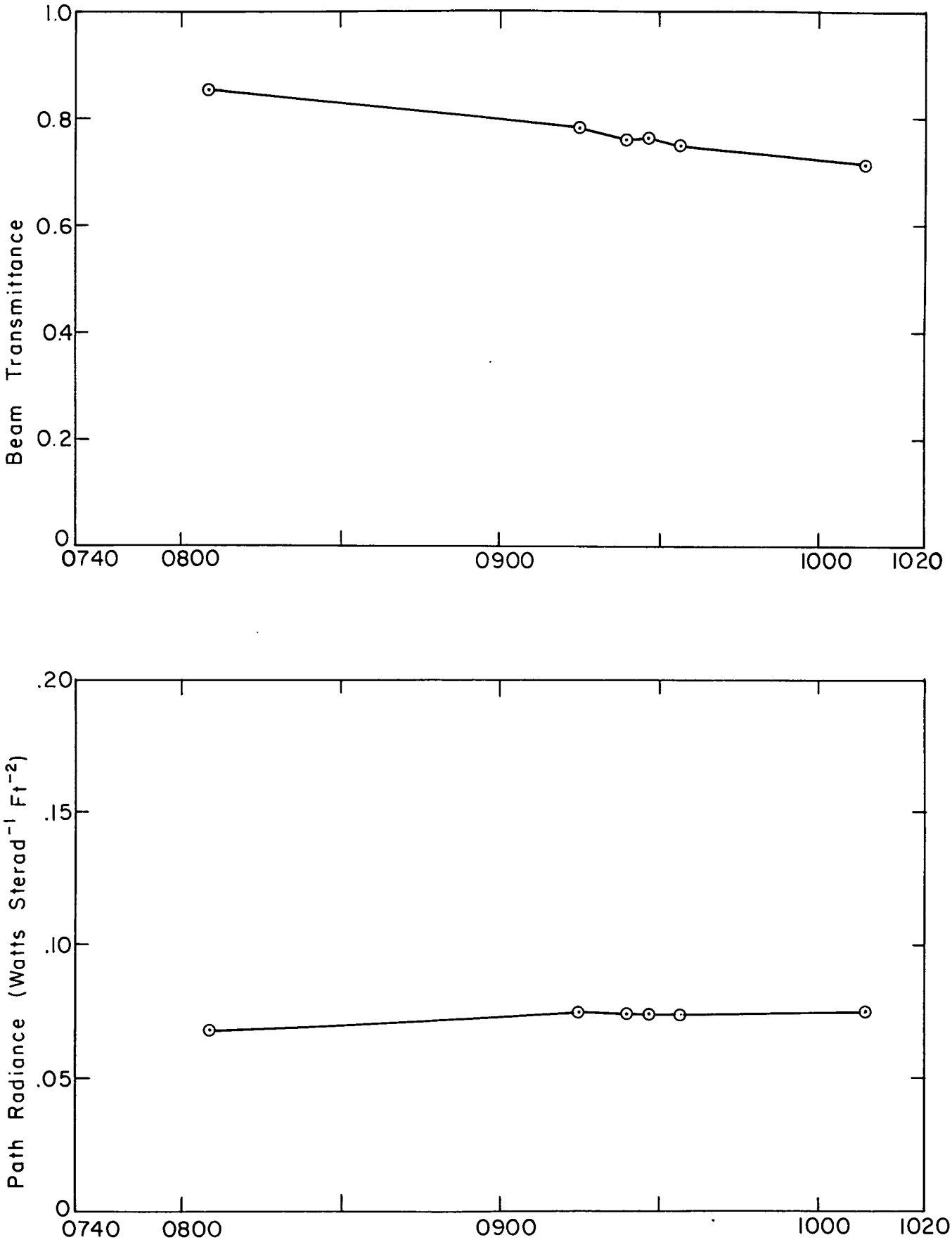

Data of 12 September 1962 Figure 17

TABLE XI

DATE OF 12 September 1962

AIRCRAFT ALTITUDE (FEET)	EASTERN STANDARD (TIME)	BEAM TRANSMIT-TANCE	PATH RADIANCE $\left(\frac{\text{WATTS}}{\text{FT}^2}\right)$	IRRADIANCE $\left(\frac{\text{WATTS}}{\text{FT}^2}\right)$	CONTRAST TRANSMITTANCE			BAR RESOLUTION CONTRAST TRANSMITTANCE 0.801 and 0.005
					TERRAIN BACKGROUND REFLECTANCE OF 0.0585 *	WHITE BACKGROUND REFLECTANCE OF 0.801	BLACK BACKGROUND REFLECTANCE OF 0.005	
PREFLIGHT	0805	0.853	0.0674	3.90	0.478	0.926	0.0728	0.864
23 400								
35 500	0915	0.782	0.0744	4.30	0.457	0.920	0.0671	0.853
42 500								
50 000	0924	0.761	0.0739	4.50	0.463	0.922	0.0687	0.856
42 500	0928	0.765	0.0740	4.55	0.466	0.923	0.0696	0.858
35 500	0934	0.750	0.0736	4.66	0.469	0.924	0.0702	0.858
23 400								
POSTFLIGHT	1009	0.712	0.0755	5.35	0.484	0.928	0.0743	0.867

*Weighted arithmetic average of estimates by Cornell Aeronautical Lab. from aerial photographs on basis of atmospheric correction factor from 7 September 1962.

APPENDIX

Visibility Laboratory
University of California
Scripps Institution of Oceanography
San Diego 52, California

EARTH-TO-SPACE CONTRAST TRANSMITTANCE MEASUREMENTS FROM GROUND STATIONS

Jacqueline I. Gordon, James L. Harris
and
S. Q. Duntley

BuShips Contract NObs-84075
Assignment No. 3
Project S F018 02 01
Task 0538

January 1963
SIO Reference 63-2

Approved for Distribution:

S. Q. Duntley

S. Q. Duntley, Director
Visibility Laboratory

EARTH-TO-SPACE CONTRAST TRANSMITTANCE MEASUREMENTS FROM GROUND STATIONS

Jacqueline I. Gordon, James L. Harris
and
S. Q. Duntley

INTRODUCTION

The ability of astronauts or satellite-borne cameras to see land masses, coast lines, or lesser objects on the surface of the earth depends upon the apparent contrast C_r of the object as viewed from orbital altitude. This, in turn, is governed by the object's inherent contrast C_o, the inherent luminance ${}_bB_o$ of its background, the transmittance T_r of the atmosphere for image-forming light, and the path luminance B_r^* (the sunlight and skylight scattered into the path of sight). Knowledge of these properties of the target, its background, the atmosphere and its lighting enable apparent contrast to be calculated by means of Eq. (1). Thus,

$$C_r = C_o \left[\frac{{}_bB_o T_r}{{}_bB_o T_r + B_r^*} \right]. \qquad (1)$$

The expression enclosed by brackets is the contrast transmittance of the path of sight.

This report describes a method believed to be capable of providing input data for Eq. (1) on the basis of optical measurements made from ground stations.

THEORY

Equation (1) is obtained by combining Eqs. (4) and (7) on pages 500 and 501, respectively, of the paper entitled "Image Transmission by the Troposphere," a reprint of which is incorporated as an appendix to this report in order to provide more complete definitions of the symbols used and a discussion of the concepts which underlie the equations.

All of the quantities in Eq. (1) depend upon the inclination of the path of sight (i.e., the zenith angle) and its azimuth relative to that of the sun. The notation explained in Appendix A provides for this by means of bracketed modifiers following each symbol; thus $C_r(5, 160, 180)$ could be written to denote the apparent contrast of an object at slant range r as seen by an observer or camera stationed at an altitude of 5 miles looking steeply downward along a path of sight depressed 160° from the zenith in an azimuth 180° from the sun, i.e., away from the sun. The altitude of observers above the atmosphere is denoted by the infinity sign ∞, since apparent contrast, transmittance, and path radiance have a single (limiting) value at any observer altitude above the atmosphere; thus, from orbit apparent contrast is written $C_r(\infty, 160, 180)$ for the same path of sight. In general, apparent contrast is written $C_r(z,\theta,\phi)$, where z is the altitude of the camera or observer. For a vertically downward view from orbit this becomes $C_r(\infty, 180, 0)$. The Appendix should be consulted for further details concerning notation and definitions. Equation (1) may now be written in a more

explicit manner. Thus,

$$C_r(\infty,\theta,\phi) = C_o(z_t,\theta,\phi) \left[\frac{{}_bB_o(z_t,\theta,\phi)\ T_\infty(\infty,\theta)}{{}_bB_o(z_t,\theta,\phi)\ T_\infty(\infty,\theta) + B_r^*(\infty,\theta,\phi)} \right] \quad (2)$$

where z_t denotes the altitude of the terrain feature or "visual target."

The beam transmittance, $T_\infty(\infty,180)$, can be readily measured by means of a solar transmissometer such as that illustrated by Fig. 1. Path luminance, $B_r^*(\infty,\theta,\phi)$, for downward paths of sight through the atmosphere can be determined from specially instrumented aircraft, but it cannot be measured directly from the ground. A primary concern of this report is, therefore, the development of an indirect method for obtaining the needed values of path luminance from ground-based measurements and certain corollary data.

It will be clear in the next section of this report that the key to the indirect method is an observed constancy in the directional pattern of equilibrium luminance data $B_q(z,\theta,\phi)$ obtained during flights conducted by the Visibility Laboratory in 1955-58 using a specially instrumented B-29 aircraft supplied to the Laboratory by the U. S. Air Force under Task 76222 of Air Force Project 7621 at the Geophysics Research Directorate of the Air Force Cambridge Research Laboratories. Development of the method to be described in this report would not have been possible without the data obtained in the course of these airborne optical experiments which were conducted with Air Force funding under Contract NObs-72092 with the Bureau of Ships. Renewed experiments of the same type are planned

for the near future in a C-130 aircraft now being instrumented for use by the Laboratory for the same Air Force project. Data expected to be obtained with the new aircraft should serve to test the observed constancies over a wider range of conditions than have been measured up to now, test the predictions of the new method, and ascertain the gamut of atmospheric and lighting conditions to which it is applicable.

Effective Equilibrium Luminance

The concept of equilibrium luminance (or radiance) is explained on page 502 of the Appendix. Briefly, for each segment of every path of sight in any lighted atmosphere there is an equilibrium luminance which will be transmitted unchanged because the loss (attenuation of image-forming light) is exactly counterbalanced by the gain due to the scattering of sunlight and skylight toward the observer. Equilibrium luminance is a point function of position and direction and in any real atmosphere it varies from point-to-point throughout every path of sight. Data from the B-29 flights, however, indicate that equilibrium luminance varies much less rapidly along the path of sight than do other optical parameters. For example, Fig. 5 on page 503 in Appendix A shows that, in this instance, the equilibrium luminance associated with a nearly horizontal path of sight was virtually independent of altitude despite wide variations in scattering and attenuation. Constancy of equilibrium luminance was commonly observed throughout the B-29 data. This suggests that, as an approximation, an effective

equilibrium luminance for each path of sight can be defined as follows:

Equilibrium Luminance in an Optical Standard Atmosphere. An atmosphere having its composition identical at all altitudes except for the number of particles per unit of volume has been called an "optical standard atmosphere." Although certain consequences of the laws of thermodynamics probably make the occurrence of a true optical standard atmosphere impossible, it is instructive, nevertheless, to consider it as a mathematical model. In an optical standard atmosphere the equilibrium luminance $B_q(z,\theta,\phi)$ is rigorously independent of altitude and is connected with the path luminance and the beam transmittance $T_r(z,\theta)$ by the relation

$$B_r^*(z,\theta,\phi) = B_q(z,\theta,\phi)\left[1 - T_r(z,\theta)\right]. \tag{3}$$

Effective Equilibrium Luminance in a non-Standard Atmosphere. In view of the experimental finding that equilibrium luminance is virtually independent of altitude under most clear weather conditions, let an effective equilibrium luminance for any path of sight be defined by an equation of the same form, that is to say,

$$B_r^*(z,\theta,\phi) = \bar{B}_q(z,\theta,\phi)\left[1 - T_r(z,\theta)\right]. \tag{4}$$

In the special case of a path of sight through the entire atmosphere from ground-to-space, Eq. (4) becomes

$$B_\infty^*(\infty,\theta,\phi) = \bar{B}_q(\infty,\theta,\phi)\left[1 - T_\infty(\infty,\theta)\right]. \tag{5}$$

Effective equilibrium luminance has been calculated for many paths of sight (both upward and downward), for most of the clear weather research flights made by the B-29. Typical results are shown in Figs. 2 and 3. It has been found that the magnitude of the effective equilibrium luminance was, on each occasion, of closely the same magnitude for every path of sight having the same angle from the sun. It will be noted that this statement is true despite the fact that the shape of the function depicted by the points in Fig. 2 is quite different from the shape of the function depicted by the points in Fig. 3. This observation is at the heart of the proposed method for obtaining earth-to-space contrast transmittance from ground-station measurements, for it is often possible to find upward paths of sight (θ',ϕ') having the same angle from the sun as the nearly vertical paths of sight involved in observation from satellites. Effective equilibrium luminance for the upward paths of sight can be obtained from an equation of the same form as Eq. (4) because such a path initiates only in the blackness of interstellar space so that the observed luminance of the sky is the path radiance $B^*_\infty(0,\theta,\phi)$. Thus, for the appropriate upward-looking paths of sight,

$$B^*_\infty(0,\theta',\phi') = \bar{B}_q(0,\theta',\phi') \left[1 - T_\infty(0,\theta')\right] . \qquad (6)$$

Path Radiance

If Eq. (5) is divided by Eq. (6) and the resulting expression

solved for the path radiance $B^*_\infty(\infty,\theta,\phi)$, there results

$$B^*_\infty(\infty,\theta,\phi) = B^*_\infty(0,\theta',\phi') \left[\frac{\bar{B}_q(\infty,\theta,\phi)}{\bar{B}_q(0,\theta',\phi')}\right] \left[\frac{1 - T_\infty(\infty,\theta)}{1 - T_\infty(0,\theta')}\right]. \tag{7}$$

The equality of the equilibrium luminance for paths of sight having identical angles from the sun, depicted by Figs. 2 and 3, can be expressed by the relation

$$\frac{\bar{B}_q(\infty,\theta,\phi)}{\bar{B}_q(0,\theta',\phi')} = 1 \quad . \tag{8}$$

To the extent to which Eq. (8) is true, Eq. (7) can be written

$$B^*_\infty(\infty,\theta,\phi) = B^*_\infty(0,\theta',\phi') \left[\frac{1 - T_\infty(\infty,\theta}{1 - T_\infty(0,\theta')}\right]. \tag{9}$$

Equation (9) enables the path radiance for downward-looking paths of sight from orbital altitude to be predicted from ground-station measurements.

Study of the Approximation. In order to evaluate the probable magnitude of the approximation represented by Eq. (8), effective equilibrium luminance was computed for appropriate pairs of paths from sea level to space based upon extrapolations of B-29 flight data. The right-hand member of Eq. (8) did not depart from unity by more than $\pm$ 10 percent in the case of any of these calculations, and in most cases

the departure was less than ± 3 percent, that is to say, it was within the precision of the experimental data.

VALIDATION EXPERIMENTS

Construction of an automatic data-logging equipment based upon Eq. (9) for accumulating beam transmittance and path radiance data for vertically downward paths of sight at the Visibility Laboratory is nearing completion. Meanwhile, endeavors have been made to conduct field experiments designed to test the proposed method. Three such validation experiments were planned. The first two resulted in no data and the third, under an Air Force contract, appears to have been successful although the final results are not yet available as of the date of this report.

First Experiment. The first validation experiment was cancelled by the Navy due to unfavorable weather. It was to have involved the last of the ONR STRATOLAB high altitude balloon flights. A manned balloon was to have been launched from an aircraft carrier off the coast of California in such a manner as to cause the balloon during its highest altitude float to pass approximately over San Clemente Island off the California coast. Arrangements were made for the balloon to carry a specially calibrated photometric camera with which the ocean near San Clemente Island was to have been photographed. Simultaneous low altitude photometric photographs from a low flying aircraft were planned for the ocean near San Clemente, and a system of photometers for measuring sky luminance and solar transmittance, as well as other optical parameters for atmospheric documentation

purposes, were to have been made from a ground station on the north tip of San Clemente Island. The balloon flight was delayed because of weather until a change in seasons caused an alteration in the circulation of the upper atmosphere which made the proposed balloon flight impracticable on the West Coast. The STRATOLAB operation was subsequently transferred to the Gulf of Mexico, where it was flown at a time when the Visibility Laboratory was unable to respond to the invitation of ONR to carry out the desired experiment.

Second Experiment. A second validation attempt was conducted in connection with the last of the HUGO rockets fired on the Pacific Missile Range from Pt. Mugu, California. This rocket carried a photometric camera calibrated by the Visibility Laboratory with the expectation that it would photograph the ocean in the vicinity of the Channel Islands from a near-orbital altitude. The remainder of the experiment was essentially identical with that originally planned for the STRATOLAB balloon flight. In this instance the experiment was carried out as planned but, unfortunately, the flotation and recovery equipment associated with the instrument package of the rocket failed to function so that the camera carried by the rocket was not recovered. Since this was the last firing of rockets of this class, the experiment could not be repeated.

Third Experiment. An opportunity to conduct a much more extensive series of validation experiments was offered by the Reconnaissance Laboratory of the Aeronautical Systems Division of the U.S. Air Force during the summer of 1962. Under a Reconnaissance Laboratory project, an Air Force photographic airplane routinely photographed a group of

black, grey, and white panels on the ground at Wright-Patterson Air Force Base, Ohio, throughout 1962. Photoelectric and photographic monitoring of the panels at ground level was provided during these flights so that contrast transmittance from ground to air could be obtained from the aerial photographs. Upon the request of the Air Force, the Bureau of Ships permitted the Visibility Laboratory's instrumented trailer van to be moved to Wright-Patterson Air Force Base where it was placed alongside the target panels so that solar transmittance and sky radiance could be measured using equipment in the trailer van during the Reconnaissance Laboratory flights.

Coordinated air and ground measurements were made by the Air Force and by the Visibility Laboratory during the period 22 August 1962 through 12 September 1962 on clear days potentially suitable for satellite observation of terrain features. Despite the fact that all of the days were "clear," a wide range of haze-cover conditions was encountered during the ten flights. Since these experiments were made under an Air Force contract, the results will appear in an Air Force report which is expected to issue during March 1963.

FIGURE CAPTIONS

Fig. 1. Solar transmissometer for measuring total transmittance of the path of sight from sun-to-ground; the total transmittance of paths of sight having other zenith angles can be obtained by means of air-mass correction. The transmissometer is a dual telephotometer for the simultaneous measurement of the luminance (or radiance) of (1) the sun and (2) the sky adjacent to the sun. A pinhole at the upper end of the telephotometer tube is used to form an image of the sun on an opaque aperture plate 50 cm from the pinhole and near the lower end of the telephotometer tube. The aperture plate is pierced by two pinholes separated sufficiently to produce two fields of view having their centers separated by approximately 20 minutes of arc. The dual pinholes have identical diameters such that the two fields of view are each about 3 minutes of arc in diameter.

The photometer is aimed in such a manner that an image of the sun is centered on one of the pinholes. Light from the sky about 5 minutes of arc from the limb of the sun then falls upon the second pinhole. Light from the first pinhole is conducted by means of a right-angle prism to a multiplier phototube, while light from the second pinhole is similarly delivered to the cathode of a second multiplier phototube. Filter wheels are provided in each of these channels, and these wheels have a remote-controlled mechanism for changing filters. Neutral filters are added as necessary in each channel in order to keep the photometric readings on scale. Each phototube is connected by a Sweet-type logarithmic circuit to a dual pen Brown recording potentiometer. The apparent

luminance of the sky is subtracted from the apparent luminance of the sun whenever it becomes sufficiently great to affect the latter reading; this seldom occurs under clear-weather conditions. A bore-sighted aiming telescope equipped with neutral filters provides an easy means for centering the solar image on the appropriate pinhole. The assembly is supported by a heavy metal tripod which forms an equatorial mounting of the usual astronomical type. Tracking the sun is accomplished by means of a hand-operated tangent screw, which is not visible in the photograph.

Fig. 2. Effective equilibrium luminance for many upward-looking paths of sight initiating at an altitude of 20,000 feet and terminating at an altitude of 1,000 feet. Each point plotted in Fig. 2 represents the effective equilibrium luminance of a different path of sight; all azimuths and zenith angles from 0 to 85° are represented. The data are from B-29 Flight 112, which took place on 16 May 1957 near Eglin Air Force Base, Florida. The beam transmittance for the vertical path of sight between altitudes 20,000 feet and 1,000 feet was 0.897. The solar zenith angle was 25°. These data illustrate that effective equilibrium luminance depends on angle from the sun but not appreciably upon zenith angle θ or azimuth angle ϕ.

Fig. 3. Effective equilibrium luminance for many upward-looking (circles) and downward-looking (crosses) paths of sight between sea level and 20,000 feet from data obtained using the B-29 aircraft and the Visibility Laboratory's trailer van during Flight 74 on 28 February 1956 near Eglin Air Force Base, Florida. Each point plotted in Fig. 3 represents the effective equilibrium luminance of a different path of sight; all azimuths and zenith angles from 0 to 60° and from 120° to 180° are represented. The beam transmittance for the vertical path of sight between these altitudes was 0.641. The solar zenith angle was 40°. As in the case of Fig. 2, these data illustrate that effective equilibrium luminance depends on angle from the sun but not appreciably upon θ or ϕ. This is true for both upward and downward paths of sight. The change in effective equilibrium luminance with angle from the sun is substantially less on the occasion represented by Fig. 3 than that depicted by Fig. 2. Both Figs. 2 and 3 suggest that effective equilibrium luminance changes very little with angle from the sun when the angle is large.

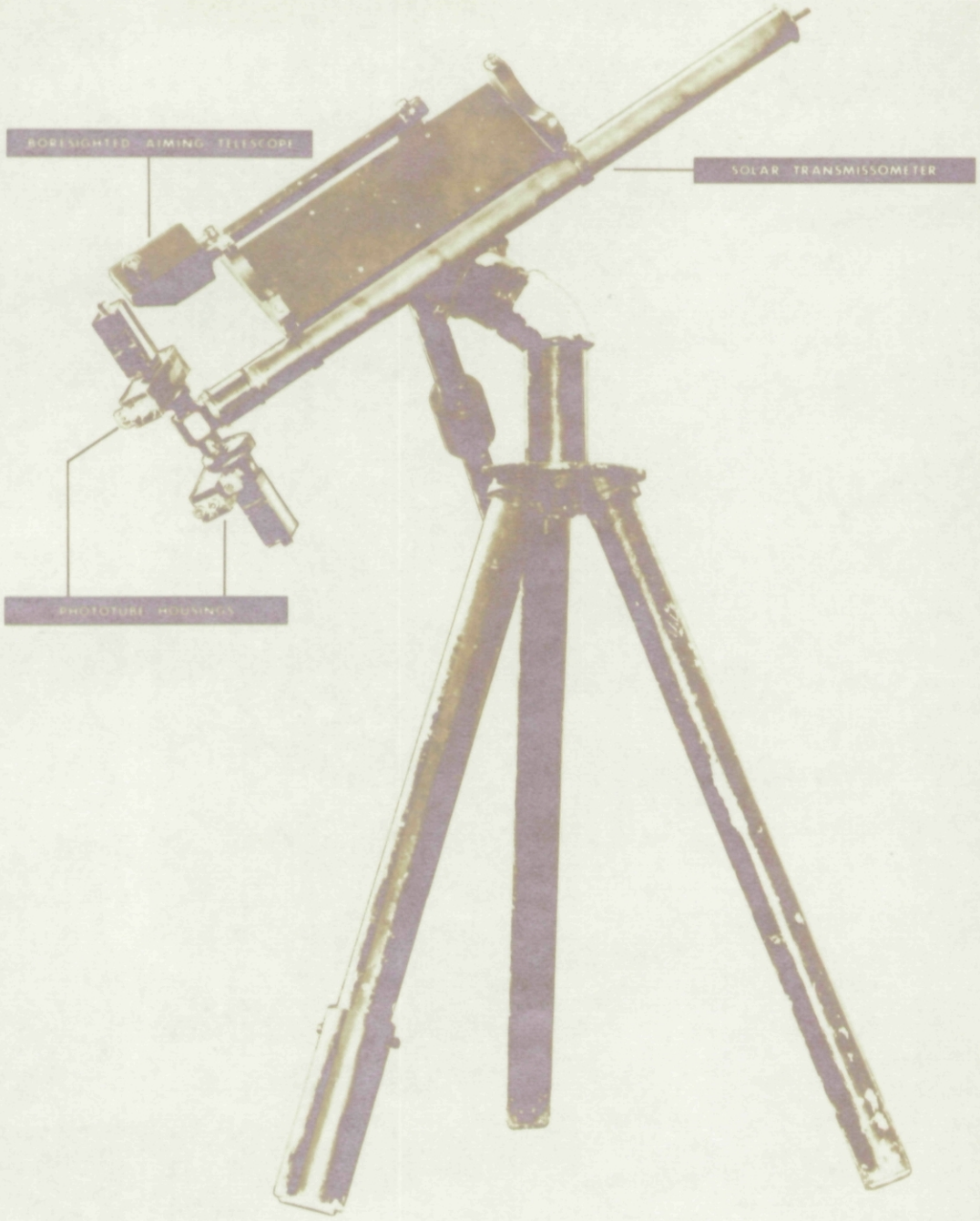
BORESIGHTED AIMING TELESCOPE
SOLAR TRANSMISSOMETER
PHOTOTUBE HOUSINGS

FIG. 1

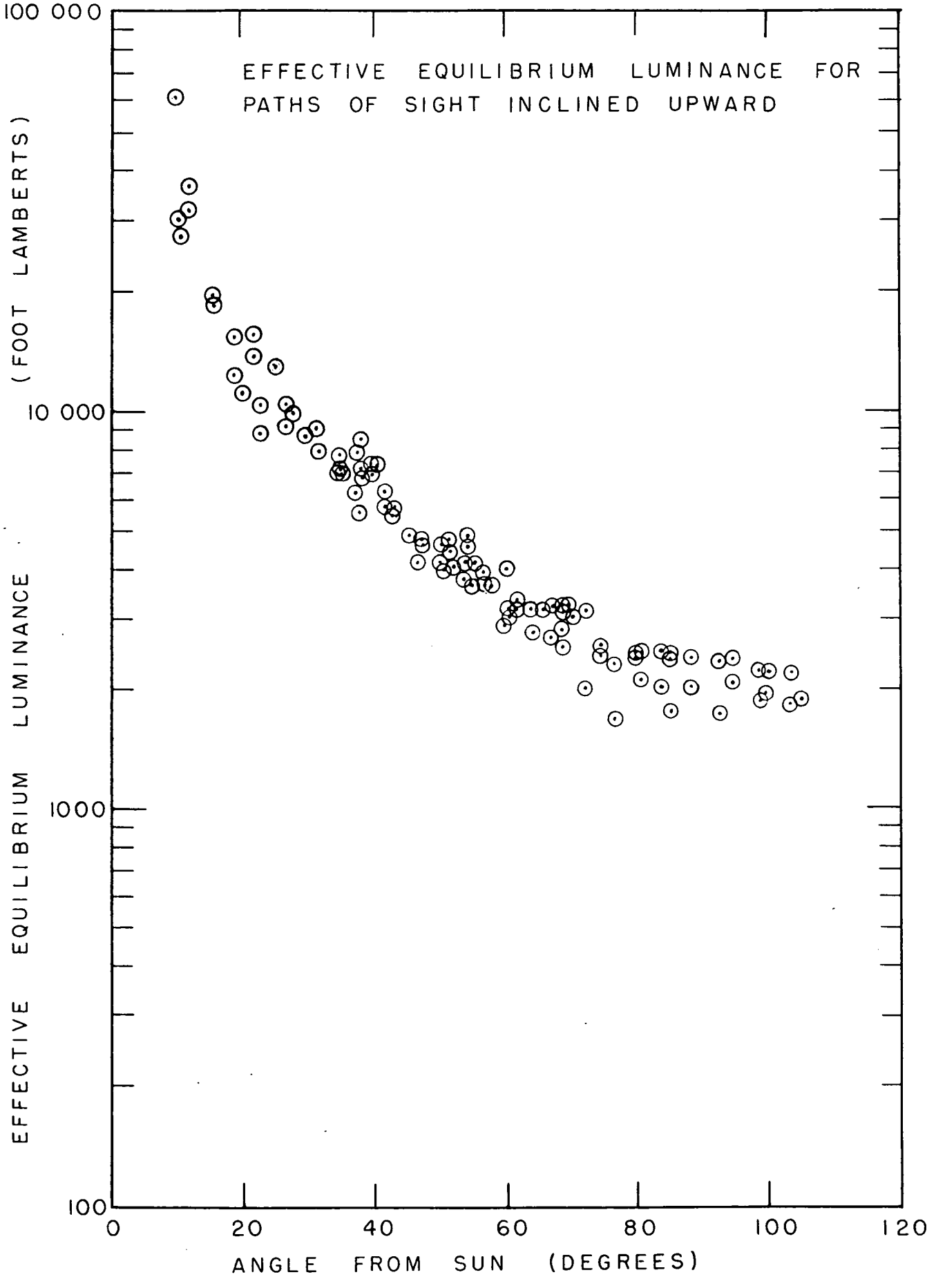
EFFECTIVE EQUILIBRIUM LUMINANCE FOR
PATHS OF SIGHT INCLINED UPWARD
EFFECTIVE EQUILIBRIUM LUMINANCE (FOOT LAMBERTS)
100 000
10 000
1000
100
0
20
40
60
80
100
120
ANGLE FROM SUN (DEGREES)

FIG. 2

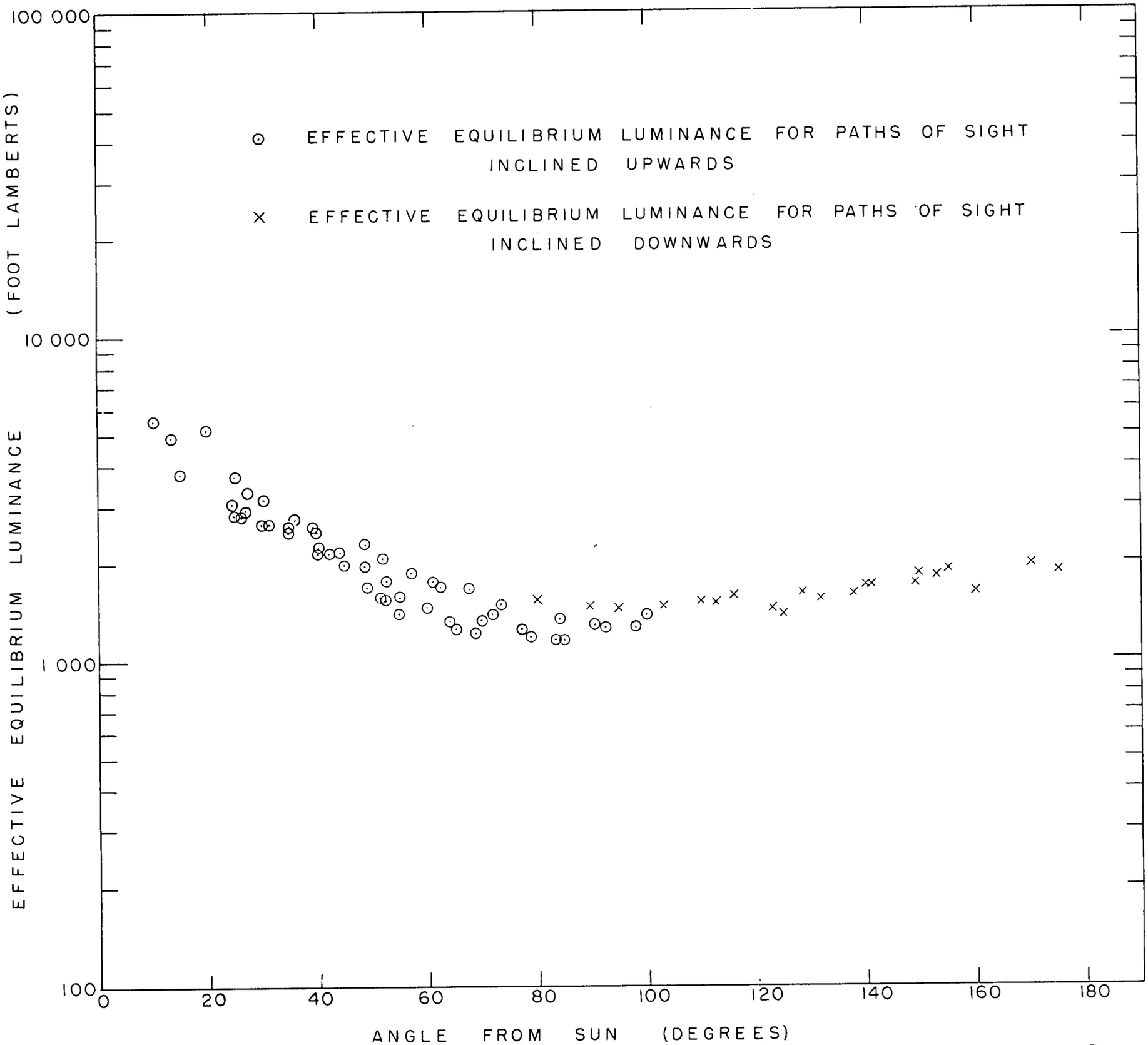
EFFECTIVE EQUILIBRIUM LUMINANCE FOR PATHS OF SIGHT INCLINED UPWARDS
EFFECTIVE EQUILIBRIUM LUMINANCE FOR PATHS OF SIGHT INCLINED DOWNWARDS
EFFECTIVE EQUILIBRIUM LUMINANCE (FOOT LAMBERTS)
100 000
10 000
1 000
100
0
20
40
60
80
100
120
140
160
180
ANGLE FROM SUN (DEGREES)

FIG. 3

Reprinted from JOURNAL OF THE OPTICAL SOCIETY OF AMERICA, Vol. 47, No. 6, 499–506, June, 1957
Printed in U. S. A.

Image Transmission by the Troposphere I*

SEIBERT Q. DUNTLEY, ALMERIAN R. BOILEAU, AND RUDOLPH W. PREISENDORFER
Scripps Institution of Oceanography,† University of California, La Jolla, California

(Received November 15, 1956)

Quantitative treatment of the apparent luminance of distant objects and the reduction of apparent contrast along inclined paths of sight through real atmospheres has been accomplished by means of optical data taken from an aircraft in flight. Sample data from a single flight are used to illustrate some of the principles involved. Correlation has been found between the humidity profile of the atmosphere and its optical properties.

INTRODUCTION

DISTANT objects are usually viewed, photographed, or televised by means of some path of sight through the atmosphere. Conventional principles of geometrical and physical optics suffice to describe the nature of the final image except for effects due to the atmosphere. In most circumstances, however, the configuration of the image and its information content is affected, often seriously, by its transmission from the object to the receiver. The atmosphere can be regarded as a transmission link in the object-to-image chain and the concomitant effect of the pertinent optical atmospheric properties can be regarded as governing its *image transmission.*

This paper is intended as the first of a series describing the results of an extensive on-going research program which has already been in progress for several years. Results from numerous theoretical and experimental investigations of image transmission phenomena are ready to be reported and further research of many kinds is in progress. Experimental results from a single flight comprise the factual content of this first paper and the equations are limited to certain general relations needed for the practical utilization of the data; this is in keeping with the scope of the oral version of the paper as presented at the Cambridge meeting of the International Commission on Optics.

The specially instrumented B-29 aircraft used to collect the data reported in this paper has, on other flights, secured data up to 30 000 ft under several different atmospheric and lighting conditions; and subsequent papers in the series will present data from these and other flights. The optical properties of the troposphere are of special interest because most viewing takes place through it. Roughly three-fourths of the atmosphere lies within the troposphere and because this lower air often contains haze, clouds, dust, and rain it seriously affects image transmission more frequently than do the higher strata. Exploration of image transmission phenomena in the stratosphere must await an opportunity to instrument a vehicle having greater altitude capability.

SOME GENERAL PRINCIPLES‡

Introduction

In the absence of appreciable atmospheric boil[1] the apparent radiance of any distant object is the sum of two independent components: (1) residual image-forming light from the object that has traversed the atmospheric path without having been scattered or absorbed; (2) radiance created by the scattering of ambient light throughout the path of sight, including sunlight, skylight, earth-shine, etc. Only the first component contains information about the object, for the second is the result of scattering processes throughout the path of sight and is, therefore, independent of the nature of the object. In this paper the image transmission of any path of sight will be specified in terms of the transmittance of the entire path and the path radiance. No theoretical model for the atmosphere is needed; consequently, nearly all restrictive assumptions are avoided and the equations can be used to describe any path of sight through all real isotropic atmospheres with any lighting condition. To be useful in practice, these equations must be supplied with data and these are becoming available as a result of the flight research program now in progress.

Notation

The notation used in this paper has been adopted with great care and on the basis of experience accumulated over many years. It is designed to fulfill many

* Presented at the Fourth Congress of the International Commission of Optics, held in Cambridge-Boston, Massachusetts, March 28–April 3, 1956. Published with financial assistance from UNESCO and the International Union of Pure and Applied Physics.

† Contribution from the Scripps Institution of Oceanography, University of California, New Series No. 921. This work has been supported by the Geophysical Research Directorate of the Air Force Cambridge Research Center and the Bureau of Ships of the U. S. Navy under contracts NObs-43356, NObs-50274, NObs-72039, and NObs-72092.

‡ The principles presented in this paper and in subsequent papers of this series were formulated in unpublished lecture notes used within the Visibility Laboratory of the Scripps Institution of Oceanography which include, generalize, and extend earlier work by the authors and others (R. W. Preisendorfer, "Lectures on photometry, hydrological optics, atmospheric optics," Fall, 1953, Vol. I).

[1] Duntley, Culver, Culver, and Preisendorfer, J. Opt. Soc. Am. 42, 877A (1952); publication of this paper is planned.

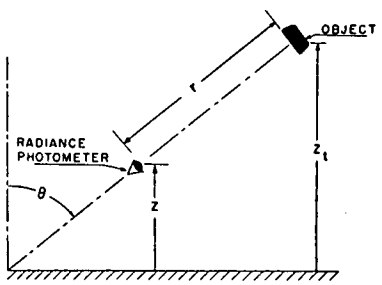

FIG. 1. Illustrating the geometry of the path of sight.

requirements: It is suited to the terrestrially-based system of altitudes and directions in which flight data must be taken and it is fully compatible with the more powerful vector notation required for the generalized theoretical treatments of image transmission and radiative transfer phenomena to follow. It is compatible also with the notation commonly used in several mathematically allied fields of physics, as for example, neutron diffusion theory. It is extendable to hydrological optics, a natural counterpart of meteorological optics, in which the authors of this paper are deeply interested.

The basic symbol employed for the spectral radiance is N, and the symbol for luminance is B. The altitude of the photometer is denoted by z, the height above mean sea level. The direction of any path of sight is specified by a zenith-angle θ and an azimuth angle ϕ, the photometer being directed upward when $0 \leq \theta < \pi/2$, as in Fig. 1; z, θ, and ϕ are always written as parenthetic attachments to the parent symbol. When the post subscript r is appended to any symbol, it denotes that the quantity pertains to a path of length r. The subscript 0 always refers to the hypothetical concept of a photometer located at zero distance from the object, as, for example, in denoting the *inherent* radiance of a surface. Pre-subscripts identify the object, thus the pre-subscript b refers to background, and t to object or visual target. Thus, the (monochromatic) *inherent spectral radiance* of an object t at altitude z_t as viewed in the direction (θ,ϕ) is ${}_tN_0(z_t,\theta,\phi)$ and the corresponding apparent radiance observed in the direction (θ,ϕ) at any other altitude z is ${}_tN_r(z,\theta,\phi)$ where $z_t=z+r\cos\theta$. A post-superscript *, or post-subscript $*$ is employed as a mnemonic symbol signifying that the radiometric quantity has been generated by the scattering of ambient light reaching the path from *all directions*. Thus $N_r^*(z,\theta,\phi)$ is the spectral path radiance observed at altitude z in the indicated direction, and $N_*(z,\theta,\phi)$ is used to denote *path function*, a quantity defined later in this paper.

The (monochromatic) *apparent spectral radiance* of any distant object t is

$$ {}_tN_r(z,\theta,\phi) = T_r(z,\theta,\phi)\ {}_tN_0(z_t,\theta,\phi) + N_r^*(z,\theta,\phi), \quad (1) $$

where the first term on the right is the residual image-forming light from the object and the second term is the path radiance due to scattering processes throughout the path. $T_r(z,\theta,\phi)$ is the spectral transmittance of the path for image-forming rays; it includes the factor $[n(z)/n(z_t)]^2$ required by geometrical optics whenever the index of refraction of the medium at the observer $[n(z)]$ differs from the index of refraction of the medium at the target $[n(z_t)]$. In the case of paths of sight through the troposphere the departure of $[n(z)/n(z_t)]^2$ from unity is negligible. The transmittance of the path is a property of the atmosphere throughout the path and is independent of the distribution of the ambient lighting; in the case of any path of sight through the troposphere it is the same for upward or downward transmissions, thus $T_r(z,\theta,\phi)=T_r(z_t,\pi-\theta,\pi+\phi)$ where $z_t=z+r\cos\theta$. Because forward scattering generally exceeds backward scattering, reversibility is not true of the path radiance $N_r^*(z,\theta,\phi)$ except for a few symmetrical lighting conditions, such as (1) horizontal paths of sight under a uniform overcast, and (2) a horizontal path at right angles to the plane of the sun provided both the radiance distributions of the sky above and the earth below the path are symmetrical with respect to the plane.

The image transmitting properties of the atmosphere can be separated from the optical properties of the object by the introduction of the *contrast* concept:

The *inherent spectral contrast* $C_0(z_t,\theta,\phi)$ of an object is, by definition,

$$ C_0(z_t,\theta,\phi) = [{}_tN_0(z_t,\theta,\phi) - {}_bN_0(z_t,\theta,\phi)]/{}_bN_0(z_t,\theta,\phi). \quad (2) $$

The corresponding definition for *apparent spectral contrast* is

$$ C_r(z,\theta,\phi) = [{}_tN_r(z,\theta,\phi) - {}_bN_r(z,\theta,\phi)]/{}_bN_r(z,\theta,\phi). \quad (3) $$

The apparent and inherent background radiances are related by the expression

$$ {}_bN_r(z,\theta,\phi) = T_r(z,\theta,\phi)\ {}_bN_0(z_t,\theta,\phi) + N_r^*(z,\theta,\phi). \quad (4) $$

Theorems

Subtracting Eq. (4) from Eq. (1) yields the relation

$$ [{}_tN_r(z,\theta,\phi) - {}_bN_r(z,\theta,\phi)] = T_r(z,\theta,\phi)[{}_tN_0(z_t,\theta,\phi) - {}_bN_0(z_t,\theta,\phi)]. \quad (5) $$

Thus, radiance differences are transmitted along inclined paths with the same attenuation as that experienced by each image-forming ray.

If Eq. (5) is divided by the apparent radiance of the background ${}_bN_r(z,\theta,\phi)$ and combined with Eq. (3), the result can be written:

$$ C_r(z,\theta,\phi) = T_r(z,\theta,\phi) \times [{}_tN_0(z_t,\theta,\phi)/{}_bN_r(z,\theta,\phi) - {}_bN_0(z_t,\theta,\phi)/{}_bN_r(z,\theta,\phi)]. \quad (6) $$

When the inherent radiance of the background is very dark, as in the case of an object at high altitude, the second term in the brackets on the right side of Eq. (6) may be negligible.

Combining Eqs. (2) and (6) yields the expression

$$C_r(z,\theta,\phi)/C_0(z_t,\theta,\phi) = T_r(z,\theta,\phi)\ {}_bN_0(z_t,\theta,\phi)/{}_bN_r(z,\theta,\phi). \quad (7)$$

The right-hand member of Eq. (7) is an expression for the *contrast transmittance* of the path of sight; it is independent of the optical properties of the object. Equation (7) is the law of contrast reduction by the atmosphere expressed in its most general form.[2]

An interesting variant of Eq. (7) formed by combination with Eq. (4) is the following expression in which *contrast transmittance* is characterized in terms of path radiance and apparent background radiance:

$$C_r(z,\theta,\phi)/C_0(z_t,\theta,\phi) = 1-[{}_bN_r{}^*(z,\theta,\phi)/{}_bN_r(z,\theta,\phi)]. \quad (8)$$

The apparent indeterminateness of Eqs. (7) and (8) when applied to the case of objects outside the atmosphere can be avoided by the use of the limiting form of Eq. (6), as follows:

$$C_r(z,\theta,\phi) = T_r(z,\theta,\phi)\ {}_tN_0(z_t,\theta,\phi)/{}_bN_r(z,\theta,\phi). \quad (9)$$

It should be emphasized that Eqs. (1) through (9) are completely general; they apply rigorously to any path of sight regardless of the extent to which the scattering and absorbing properties of the atmosphere or the distributions of lighting exhibit nonuniformities from point to point. No theoretical model of the atmosphere is involved and no restrictive assumptions have been made. The equations can be used in treating all real atmospheres and all real lighting conditions. This is in sharp distinction to treatments of the subject which are based upon theoretical models of the atmosphere which invariably involve major assumptions such as horizontal uniformity, exponential lapse rate of air density, vertical uniformity of particle size distribution, negligible earth curvature, etc.

Equation of Transfer

Image-forming light is lost by scattering and absorption in each elementary segment of the path of sight and contrast-reducing path radiance is generated by the scattering of the ambient light which reaches the segment from all directions. The quantitative description of this scattered component of path-segment radiance involves a quantity called the *path function* and denoted by the symbol $N_*(z,\theta,\phi)$, where the mnemonic subscript symbol $*$ is used both to suggest light reaching the path segment from all directions and to denote that the quantity is a point function. The parenthetical symbols (z,θ,ϕ) indicate that the path function depends upon the direction of image transmission and upon the location of the segment in the path of sight. The path function depends upon the directional distribution of the lighting on the segment due to its surroundings; it can be operationally defined in terms of the (limiting) ratio of the path radiance associated with a short path to the path length by the relation $N_*(z,\theta,\phi) = \lim(\Delta r \to 0) \times N_{\Delta r}{}^*(z,\theta,\phi)/\Delta r$. In experimental practice, the path length Δr should be sufficiently short that no change in the ratio can be detected if Δr is made shorter. Apparatus for path function measurement has been built and will be described elsewhere.

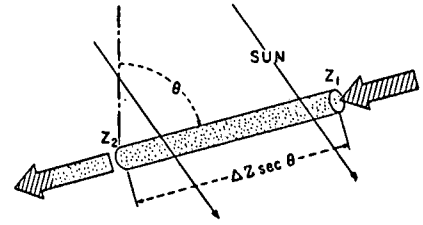

FIG. 2. Illustrating the derivation of the equation of transfer. Δz is defined as $z_1 - z_2$, so that $\Delta r = \Delta z \sec\theta$ is always non-negative. The difference $\Delta N(z,\theta,\phi)$ between output and input is $N(z_2,\theta,\phi) - N(z_1,\theta,\phi)$.

The loss in image-forming light due to attenuation by scattering and absorption within any path segment is proportional to the amount of image-forming light present; the coefficient of proportionality will be written in the reciprocal form $1/L(z)$, and $L(z)$ will be referred to as the *attenuation length*. $L(z)$ is a function of position within the path of sight; it does not depend upon the image transmission direction unless the aerosol is anisotropic, as sometimes occurs in the case of falling snow; it is independent of the manner in which the path segment is lighted by the sun or sky; it is a physical property of the atmosphere alone. Attenuation includes loss of image-forming radiance by absorption and by scattering. Absorption refers to any thermodynamically irreversible transformation of monochromatic radiant energy including, primarily, conversion of light into heat but also fluorescence phenomena, photochemical processes, etc. Attenuation by scattering results from any change of direction sufficient to cause the radiation to fall outside the summative radius of the detector mosaic.

In any path segment of length $\Delta r = \Delta z \sec\theta$, as illustrated by Fig. 2, the difference $\Delta N(z,\theta,\phi)$ between output and input radiance is attributable to a gain term $N_*(z,\theta,\phi)\Delta r$ and a loss term $N(z,\theta,\phi)\Delta r/L(z)$, so that $\Delta N(z,\theta,\phi) = N_*(z,\theta,\phi)\Delta r - N(z,\theta,\phi)\Delta r/L(z)$. This relation may be rewritten

$$\Delta N(z,\theta,\phi)/\Delta z \sec\theta = N_*(z,\theta,\phi) - N(z,\theta,\phi)/L(z). \quad (10)$$

In conformity with usage in other fields of physics Eq. (10) will be referred to as the incremental form of the *equation of transfer*. It is implicit in this equation that Δz must be taken sufficiently small so that over this interval $L(z)$ and $N_*(z,\theta,\phi)$ may be regarded as constants within the precision of experimental data.

[2] Equation (7) is a generalization of Eq. (15) on p. 183 of Q. Duntley, J. Opt. Soc. Am. 38, 179 (1948).

Equation (10) is a steady-state equation of continuity,[3] based upon the conservation of energy principle; it refers only to nonemitting atmospheres, since an additional term would be needed to represent emission of radiation in the path, as by fluorescence, recombination phenomena, particle excitation, etc. Self-radiosity within the visible spectrum appears to be of negligible importance in the troposphere. Equations (1) and (4) may be regarded as integral forms of the equation of transfer.

The equation of transfer and the concepts of attenuation length and path function share the same generality as the concepts associated with Eqs. (1) through (9): No theoretical model atmosphere has been employed; each of the equations in this paper is applicable to all real isotropic atmospheres, all lighting conditions, and all paths of sight. The use of the equation of transfer in numerical summation procedures involving experimental data will be illustrated in a later section of this paper. Only when Eq. (10) is simulated by a differential equation and an analytic integration performed does the introduction of a theoretical model for the atmosphere become necessary; this will not be done in the present paper.

Equilibrium Radiance

Many image transmission phenomena are most clearly understandable in terms of the concept of *equilibrium radiance*. This concept is a natural consequence of the equation of transfer, which indicates that some unique *equilibrium radiance* $N_q(z,\theta,\phi)$ must exist at each point such that the loss of radiance within the path segment is balanced by the gain, i.e., $\Delta N_q(z,\theta,\phi)=0$. Thus

$$0=N_*(z,\theta,\phi)-N_q(z,\theta,\phi)/L(z), \quad \text{so that}$$
$$N_q(z,\theta,\phi)=N_*(z,\theta,\phi)L(z) \tag{11}$$

and the equation of transfer (10) may be rewritten as follows:

$$\Delta N(z,\theta,\phi)/\Delta z \sec\theta=[N_q(z,\theta,\phi)-N(z,\theta,\phi)]/L(z). \tag{12}$$

Equation (11) shows that each segment of every path of sight has associated with it an equilibrium radiance, and Eq. (12) states that the average space rate of change in image-forming radiance caused by the path segment is in such a direction as to cause the output radiance to be closer to the equilibrium radiance than is the input radiance. This segment-by-segment convergence of the apparent radiance of the object to the dynamic equilibrium radiance is illustrated by the data in Fig. 6 of this paper.

[3] The equation of transfer has been generalized to the transient case, and rigorously derived for an arbitrary optical medium, using the concepts of measure theory. R. W. Preisendorfer, "A mathematical foundation for radiative transfer theory," Doctoral dissertation, U.C.L.A., May 1956. An exposition of this theory has been submitted for publication in the Journal of the Optical Society of America.

When the path of sight is horizontal and optically uniform both in terms of the composition of the aerosol and its lighting, the equilibrium radiance is identical with the apparent radiance of the horizon. The apparent radiance of distant objects inherently more radiant than the equilibrium value decreases toward the equilibrium radiance as an asymptote; conversely the apparent radiance of any dark distant object approaches the same asymptote.

Equilibrium Contrast

Many of the foregoing equations can be rewritten in terms of *equilibrium contrast*, $C_q(z,\theta,\phi)$, which is defined by the relation

$$C_q(z,\theta,\phi)=[{}_tN_r(z,\theta,\phi)-N_q(z,\theta,\phi)]/N_q(z,\theta,\phi). \tag{13}$$

Notation of the type defined by Eq. (13) enables the equation of transfer (10) to be written

$$\Delta C_q(z,\theta,\phi)/\Delta z \sec\theta=-C_q(z,\theta,\phi)/L(z) \tag{14}$$

or

$$\Delta C_q(z,\theta,\phi)/C_q(z,\theta,\phi)=-\Delta z \sec\theta/L(z), \tag{15}$$

provided that the equilibrium radiance $N_q(z,\theta,\phi)$ is constant on the segment of path under discussion. In this case the fractional change in equilibrium contrast depends only upon the ratio of the length of the path segment to the attenuation length. The negative signs throughout Eqs. (14) and (15) signify that equilibrium contrast decreases in absolute magnitude in the segment.

EXPERIMENTAL METHODS

Introduction

The apparent radiance of any distant object can be computed by means of Eq. (1) if the transmittance of the path of sight and the path radiance are calculated from experimental data. This can be done from profiles of attenuation length and path function for the path of sight by means of the relations

$$T_r(z,\theta,\phi)=[n(z)/n(z_t)]^2\prod_{i=1}^{m}\exp\{-\Delta r/L(z_i)\}$$
$$=[n(z)/n(z_t)]^2\exp\{-\Delta r\sum_{i=1}^{m}1/L(z_i)\} \tag{16}$$

and

$$N_r^*(z,\theta,\phi)=\Delta r\sum_{i=1}^{m}T_{ri}(z,\theta,\phi)N_*(z_i,\theta,\phi), \tag{17}$$

where the vertical height $|z_t-z|$ of the path is divided into m equal segments of length Δz, and $\Delta r=\Delta z \sec\theta$. $L(z_i)$ and $N_*(z_i,\theta,\phi)$ are the mean values of L and N_* in the ith segment. $r_i=(i-1)\Delta r$, $i=1,\cdots,m$.

Attenuation Profile

An experimental technique for measuring the vertical profile of attenuation length in horizontally uniform atmospheres has been devised around an air-borne version of an instrument based upon principles described earlier.[4,5] Figure 3 shows this attenuation meter mounted on the B-29 aircraft used by the Visibility Laboratory in its flight research program. The optical system is shown diagrammatically in Fig. 4. The forward telephotometer is directed toward the horizon and measures the equilibrium radiance of the horizontal path of sight in the direction of flight of the aircraft. The rear telephotometer measures the radiance of a path of unit length; this is numerically equal to the path function. The attenuation length is the ratio of the equilibrium radiance to the path function, as shown by Eq. (11). Recording potentiometers within the aircraft record the outputs of both telephotometers as well as their ratio.

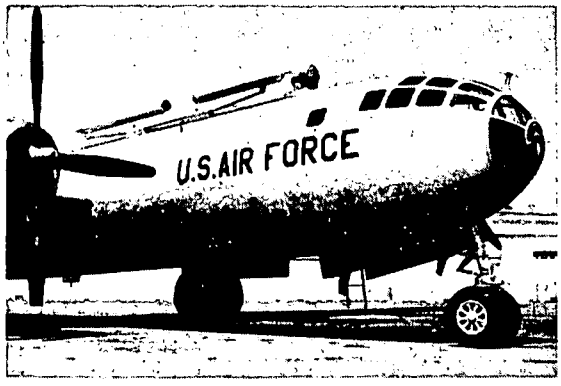

FIG. 3. Specially instrumented B-29 aircraft used to collect the data presented in this paper. The long cylindrical apparatus on top of the fuselage is the *attenuation meter*, shown schematically in Fig. 4. The smaller cylindrical device which appears slightly forward of the attenuation meter is the sky-scanning telephotometer. It consists of an end-on type multiplier phototube mounted at the focal point of a parabolic front-surfaced mirror 12 in. diam. Scanning is accomplished automatically by means of a turret and trunion mounting; scanning time for the entire hemisphere is 90 sec. Field of view, adjustable by means of interchangeable field stops, was circular, 5° in angular diameter in the case of the data shown in Fig. 6. Sensitivity is sufficient to map even the darkest high-altitude night skies. Spectral response is controlled by absorption filters. A similar (downward-viewing) telephotometer is mounted beneath the aircraft but is not shown by this photograph.

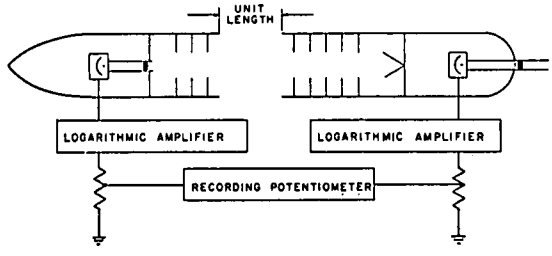

FIG. 4. Schematic diagram of the air-borne attenuation meter. The forward photoelectric telephotometer measures the equilibrium radiance; the rear telephotometer measures the radiance of a path of unit length. The latter radiance is numerically equal to the horizontal path function in the direction of flight. Multiplier phototubes and Sweet-type logarithmic circuits enable direct recording of the ratio of these radiances, i.e., of the attenuation length [see Eq. (11)]. Wind-tunnel tests of the aerodynamic design showed ambient pressure throughout the unit path. Light trap design, stray-light treatment, and photoelectric sensitivity are sufficient to enable measurement of attenuation lengths up to 200 nautical miles when the phototube spectral sensitivity is rendered photopic by means of absorption filters.

[4] S. Q. Duntley, U. S. Patent No. 2,661,650.
[5] S. Q. Duntley, J. Opt. Soc. Am. 39, 630A (1949).

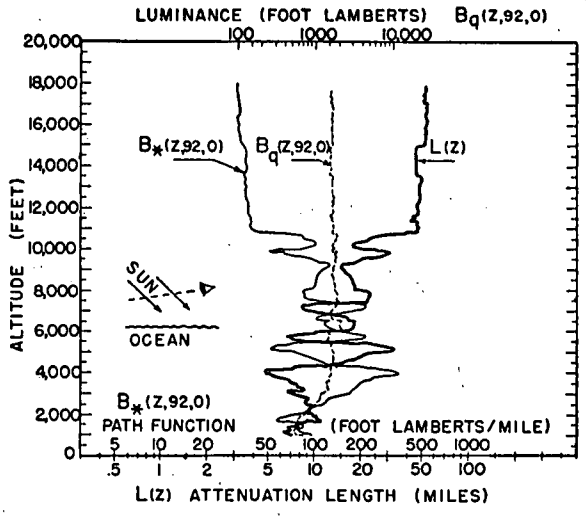

FIG. 5. Measured profiles of path function and attenuation length over the Atlantic Ocean off the coast of Florida, March 10, 1956. Flight 77. Sun position: zenith angle = 48°, azimuth = 140° clockwise from true north. Path function: zenith angle $\phi = 92°$; azimuth $\theta = 0°$ from the plane of the sun. Sky condition: cloudless, blue. Approximately 36 hr after the passage of a major front. Very light ground haze with top at 4000 ft. The profile of equilibrium luminance was computed by means of Eq. (11).

Despite the use of multiplier phototubes, the low level of radiance produced by scattering processes in clear high altitude air precluded the use of narrow-band interference or absorption filters in the airborne attenuation meter. Because it was not possible to measure the spectral radiances called for by the equations given in this paper, each phototube was carefully corrected by means of specially constructed absorption filters to measure luminous quantities. For reasons of rigor the equations in this paper are written with the symbol N, denoting spectral radiance, but it will be understood that these same equations have been used with N replaced by B, denoting luminance, in the treatment of the illustrative data shown in Figs. 5 through 8.

During the flight for which data is given in this paper, the aircraft maintained a constant (southerly) heading and a fixed attitude which held the attenuation meter pointed at the desired portion of the horizon sky while making a controlled, rapid descent from 18 000 ft to 1000 ft at a rate of approximately 1500 ft per min. The resulting profiles of path function, equilibrium luminance, and attenuation length are shown in Fig. 5.

It will be noted that the equilibrium luminance (horizon luminance) was nearly independent of altitude. Repeated descents have demonstrated that the major details of these curves are repeatable.

The transmittance of any inclined path of sight having terminal altitudes between 1000 and 18 000 ft can be calculated from the attenuation profile in Fig. 5 by means of equations corresponding to Eq. (16).

Path Function Profiles

The aircraft is not equipped for the direct measurement of path functions for vertical and inclined paths of sight. It is capable, however, of measuring the radiance of the sky in any direction, above or below, during flight. A photoelectric telephotometer is located in a trunion mounting on top of the fuselage near the forward end of the attenuation meter, as shown in Fig. 3. This instrument performs an automatic scan of the entire sky above the aircraft in approximately 90 sec. Another telephotometer in a fixed vertical mount provides a continuous record of the radiance of the zenith during the controlled rapid descent described in the preceding section. A corresponding pair of telephotometers is mounted on the bottom of the fuselage. Figure 6 shows zenith luminance data secured by the fixed telephotometer during the same descent to which Fig. 5 applies. Similar profiles of sky luminance for any upward path of sight inclined at angles θ, ϕ can be constructed from the record of the sky-scanning telephotometer, which is designed to be operated continuously during the descent.

The profile of the path function for any path of sight can be calculated from the sky radiance profile and the attenuation profile by means of Eq. (10) after rearrangement as follows:

$$N_*(z,\theta,\phi)=\Delta N(z,\theta,\phi)/\Delta z\,\sec\theta+N(z,\theta,\phi)/L(z). \quad (18)$$

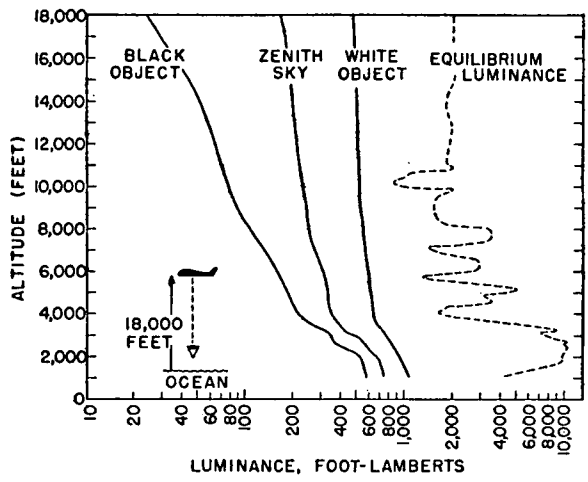

FIG. 6. Measured profile of the luminance of the zenith sky. Flight 77. Calculated profiles of the apparent luminance of black and white objects at 18 000 ft. Calculated profile of vertical equilibrium luminance.

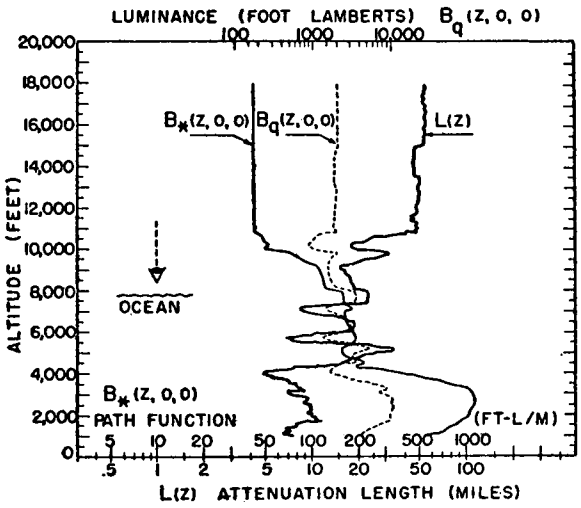

FIG. 7. Calculated profiles of vertical path function and vertical equilibrium luminance. Flight 77. The profile of attenuation length is identical with that in Fig. 5.

Figure 7 shows the result of such a calculation for the vertical path of sight which corresponds with the zenith luminance profile given in Fig. 6.

Equilibrium Radiance Profiles

An expression for the equilibrium radiance for each element of any path of sight can be found by combining Eqs. (11) and (18) as follows:

$$N_q(z,\theta,\phi)=L(z)(\Delta N(z,\theta,\phi)/\Delta z\,\sec\theta)+N(z,\theta,\phi). \quad (19)$$

Figure 6 shows the result of the use of Eq. (19) for a calculation of the equilibrium luminance profile for the upward vertical path of sight; the same profile appears in Fig. 7.

In every case the radiance of the sky $N(z,\theta,\phi)$ as observed from any altitude z is the path radiance generated by the portion of the path above the observer. That is, $N(z,\theta,\phi)=N_\infty{}^*(z,\theta,\phi)$, where $0\leq\theta<\pi/2$. Because $N(z,\theta,\phi)=0$ outside the atmosphere (except for light from the stars) and $N(z,\theta,\phi)>0$ within, it follows from Eq. (19) that the equilibrium radiance exceeds the apparent radiance of the clear sky and, therefore, the measured radiance of a clear sky increases as the photometer descends.

When clouds are present or when the image transmission direction is upward, the apparent radiance reaching any particular path segment may exceed the equilibrium radiance for that segment, so that a decrease of apparent radiance is possible. In such cases it often happens that the apparent radiance of highly radiant objects decreases while that of objects of small inherent radiance increases. Illustrative data for upward-transmitting paths of sight are planned for presentation in a subsequent paper.

Profiles of Apparent Object Luminance

Profiles of the apparent luminance of any specific object can be calculated for any path of sight provided that the inherent luminance of the object in the direction of interest is known. Two such profiles appear in Fig. 6; they refer to hypothetical "black" and "white" objects, respectively, located at a fixed altitude of 18 000 ft and viewed from directly below on the occasion to which the data in this paper applies. The profiles were calculated by means of Eq. (1). Alternatively, they could have been generated step-wise by successive applications of either Eq. (10) or Eq. (12). The complexity which characterizes the attenuation, path function, and equilibrium luminance profiles is scarcely noticeable in these vertical profiles of apparent object luminance. In the case of paths of sight inclined at large zenith angles, however, the object luminance profiles exhibit the complexities due to atmospheric structure much more prominently.

Profiles of Apparent Contrast

Figure 8 shows profiles of apparent object contrast generated by means of Eq. (3) from the apparent luminance profiles in Fig. 6. The same profiles could have been generated by use of the Eq. (7).

METEOROLOGICAL CORRELATIONS

The complex profiles of attenuation length and path function can only be the result of sharply defined layers of scattering particles. Repeated descents have demonstrated that the major features of the profiles are reproducible in space and time; the layers must, therefore,

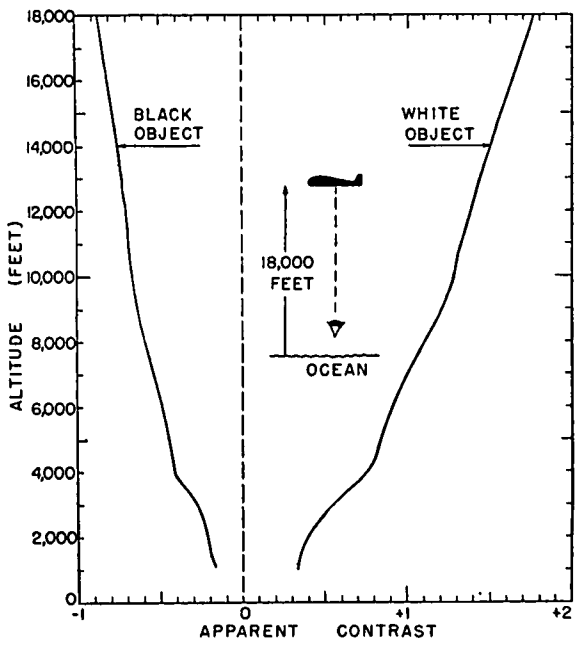

FIG. 8. Calculated profiles of the apparent contrast of black and white objects at 18 000 ft. Flight 77.

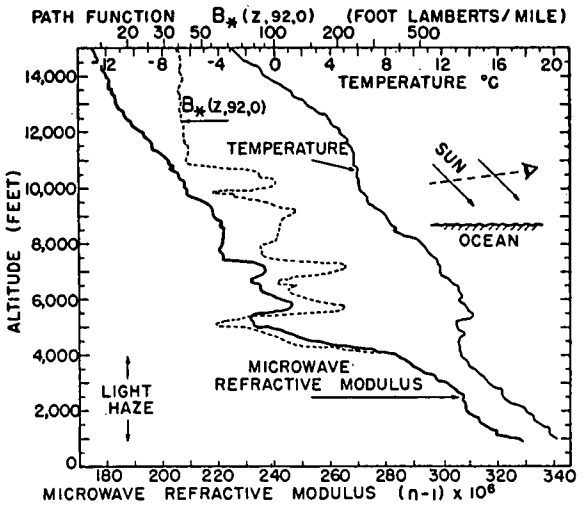

FIG. 9. Profiles of microwave refractive modulus, path function, and free air temperature. Flight 77. Correlations between the profiles of microwave refractive modulus and path function can be noted.

be horizontal strata of great extent which characterize the air mass. Such strata must also be observable in terms of nonoptical meteorological phenomena. Initial attempts to discover correlations with the temperature and humidity profiles produced routinely by the meteorological services from radiosonde observations met with failure. This was attributed to the long time constant associated with the humidity sensing elements carried by the balloons. It was believed necessary to measure the humidity profile during the controlled rapid descent of the B-29 with equipment having a fractional second time constant in order to record faithfully the presence of strata only a few feet in thickness. This was accomplished by means of an airborne microwave refractometer[6] of the type described by Crain and Deam.[7] The microwave refractive index recorded by this instrument is governed primarily by the water vapor concentration in the atmosphere; it is related to pressure, temperature, and the partial pressure of water vapor by an equation derived by Debye and discussed by numerous authors in connection with microwave propagation.[8] An expression for the partial pressure of water vapor obtained from the usual microwave approximation of Debye's equation is:

$$\epsilon = \frac{(\text{microwave refractive modulus})(\text{Kelvin temp.})^2}{(77.6)(4810)} - \frac{(\text{total pressure})(\text{Kelvin temp.})}{4810}.$$

[6] The authors are indebted to Mr. Thomas J. Obst, Director of Range Development, Patrick Air Force Base, for suggesting the use of the microwave refractometer and for arranging for the availability of this equipment for the flight experiment described in this paper.

[7] C. M. Crain and A. P. Deam, Rev. Sci. Instr. 23, 149 (1953).

[8] E. K. Smith, Jr., and S. Weintraub, J. Research Natl. Bur. Standards 50, 39 (1953).

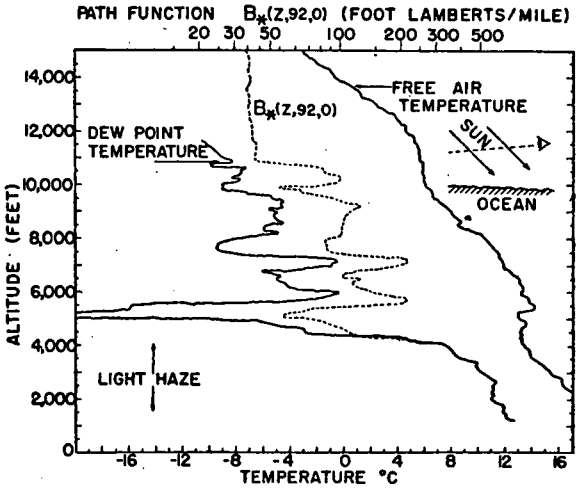

FIG. 10. Profile of dew point temperature calculated by means of Debye's equation from the profile of microwave refractive modulus in Fig. 9. Profiles of path function and free air temperature are identical with those in Fig. 9. Correlations between profiles of dew point temperature and path function are obvious.

In this equation ϵ is in millibars, the Kelvin temperature is of the stratum, the total pressure is in millibars, and the *microwave refractive modulus* of the stratum for microwaves is defined by the expression $(n-1)\ 10^6$, where n is the refractive index of the stratum.

An Air Force C-131 equipped with a microwave refractometer flew in formation with the B-29 throughout the descent during which the optical data reported in this paper was secured. The resulting profile of microwave refractive modulus is shown in Fig. 9. The profile of horizontal path function from Fig. 5 also appears in Fig. 9 for purposes of comparison.

Debye's equation was used to calculate a humidity profile from the microwave data. This profile, expressed in terms of dew-point temperature, is given in Fig. 10. The close correlation between humidity and path function is obvious.

The following speculations on the reasons for the observed correlation are offered: In terms of visible light water vapor exhibits virtually no absorption and it contributed only molecular scattering, the magnitude of which is too small to be responsible for the observed effects. The atmosphere invariably contains, however, suspended material such as sea-salt ions, silica, ammonia, or oxides of nitrogen and sulfur which can form condensation nuclei for water droplets. A tenuous haze of these tiny droplets will form in any stratum having a water vapor content above some critical minimum. These droplets will grow until the vapor pressure just outside the curved surface of the drop equals the partial pressure of water vapor in the surrounding air.[9] Liquid droplets ranging from 4×10^{-7} to more than 10^{-4} cm are known to be present in the atmosphere.[10] In the case of spherical water droplets small in diameter compared with a wavelength of light that component of the scattering coefficient which is due to droplets increases as the sixth power of their diameter,[11] assuming the number of droplets per unit of volume to remain fixed. In view of this, the observed correlation between the path function and the humidity within tenuous haze layers appears to be understandable.

ACKNOWLEDGMENTS

The number of individuals involved in an experimental program of the complexity, scope, and duration of the flight research partially described by this paper is too great to be listed properly here. Special mention should be made, however, of the technical contributions of Brig. Gen. Victor A. Byrnes, USAF, through whose efforts the program was initiated; Lt. Col. George E. Long, USAF; Major Joseph X. Brennan, USAF; and research pilot Capt. Robert L. Baron, USAF. Important contributions to the detailed design of the apparatus were made by John M. Hood, Roswell W. Austin, W. Joseph Woodside, Thomas H. Glenn, Romuald Anthony, Merril D. Hobt, and David J. A. Hooton.

[9] W. E. K. Middleton, *Vision through the Atmosphere* (Toronto Press, Toronto, 1952), Chap. 3.

[10] C. Junge, *Nuclei of Atmospheric Condensation*, Compendium of Meteorology (American Society for Metals, Cleveland, 1951).

[11] Lord Rayleigh, Proc. Roy. Soc. (London) **A90**, 219 (1914).